

Linear and nonlinear light scattering and absorption in free-electron nanoclusters with diffuse surface: General considerations and linear response

S. V. Fomichev^{1,2,*} and W. Becker^{2,†}¹*Russian Research Center “Kurchatov Institute,” Institute of Molecular Physics, Kurchatov Place 1, 123182 Moscow, Russia*²*Max-Born-Institut für Nichtlineare Optik und Kurzzeitspektroskopie, Max-Born-Straße 2A, 12489 Berlin, Germany*

(Received 29 March 2010; published 29 June 2010)

Both linear and nonlinear scattering and absorption of a laser pulse by spherical nanoclusters with free electrons and with a diffuse surface are considered in the collisionless hydrodynamics approximation. The developed model of forced collective motion of electrons confined to a cluster permits one consistently to introduce into the theory all the sources of nonlinearity, as well as the inhomogeneity of the cluster near its boundary. Two different perturbation theories corresponding to different laser intensity ranges are developed in this context, and both cold metal clusters and hot laser-heated or -ionized clusters are considered within the same approach. In the present article, after developing the full nonlinear model, the linear response to the laser field of the free-electron cluster with diffuse surface is investigated in detail, especially the properties of the linear Mie resonance (width and position). Under certain conditions, depending on the various cluster parameters secondary resonances are found. The properties of resonance-enhanced third-order harmonic generation and nonlinear laser absorption and their dependence on the shape of the diffuse surface will be presented separately.

DOI: [10.1103/PhysRevA.81.063201](https://doi.org/10.1103/PhysRevA.81.063201)

PACS number(s): 36.40.Gk, 42.65.Ky, 52.38.Dx, 73.22.Lp

I. INTRODUCTION

Since the pioneering work of Lord Rayleigh [1], the linear electromagnetic response of small metallic particles has been extensively studied, especially scattering and absorption of the applied electromagnetic field by particles with radii smaller than the wavelength of the applied field. The next important contribution to the theory was made by Mie [2] who discovered the surface plasmon modes (the Mie resonances) effectively excited in small metal particles by the electromagnetic field. An incomplete list of subsequent progress in this domain includes Refs. [3–23]. Some of these works [3,6,17,18] already noted the important role of the diffuseness of the particle surface for the properties of the dipole Mie resonance in small metal particles. This holds, in particular, for the explanation of the red shift of the Mie-resonance frequency in simple metal clusters (the term, which we will use hereafter for nano-sized particles) with respect to its value for a steplike cluster boundary. Obviously, the role of the diffuseness of the cluster surface increases with decreasing cluster radius, and for small metal clusters or, more generally, free-electron nanoclusters it may be decisive even for the linear electromagnetic cluster response, not to speak of the nonlinear response, for which the role of the cluster surface is generally much more important. However, even for the linear response there are still insufficiently studied points concerning the role of the diffuse surface for such small nanoclusters. On the other hand, less attention has been paid so far to the nonlinear electromagnetic response of nanoclusters, and, in particular, to third-harmonic generation (THG) by the cluster. The latter is becoming increasingly important now in practical applications, in particular, in the medical-biological area [24–26].

The first theoretical works on the nonlinear electromagnetic cluster response [27,28] appeared more than 100 years after Lord Rayleigh’s seminal article [1]. Thereafter, this was extensively investigated with respect to harmonic generation by the cluster [29–47] as well as nonlinear laser absorption [48–55]. References [32–34] noted the important role of the cluster surface in the process of THG. A simple model of THG by a small metallic cluster was developed in Refs. [35–37], which involved a noncompressible electron cloud oscillating under the action of the applied electromagnetic field with respect to the positively charged ion core. In this model, the collective electron motion near the sharp-edged cluster surface is responsible for THG, and the effect is proportional to the gradient of the electron density on the surface of the cluster, assuming that the electron density extends to regions outside the cluster. This model permits one qualitatively to understand the mechanism of harmonic generation in free-electron clusters, including its resonant enhancement near the third-order resonance of the laser field with the dipole Mie resonance, and to evaluate the THG yield. Later, the results obtained within this simple model about resonance-enhanced THG in the process of collective electron motion in clusters was confirmed experimentally for cold metal (gold and silver) clusters [56–58], for hot laser heated/ionized argon clusters [59], as well as in computer simulations by different methods.

In this article, a collisionless hydrodynamic model is developed in order to explore both the linear and the nonlinear electromagnetic response of small nanoclusters with free electrons and with a diffuse surface to an incident laser field. It permits us properly to take into account all the nonlinearities that are naturally present in the hydrodynamic equations for the collective motion of an electron gas in the restricted volume of a nanocluster, as well as the nonuniformity of the ion and electron density in the diffuse surface of the nanocluster. Within the same approach, we consider cold metal clusters, which also may be embedded in dielectric surroundings, and arbitrary hot clusters laser-heated/ionized by a strong pump

*fomichev@imp.kiae.ru; Also at Moscow Institute of Physics and Technology, 141700 Dolgoprudny, Moscow Region, Russia.

†wbecker@mbi-berlin.de

laser pulse, which may be positively charged due to outer ionization. The one-dimensional version of this model was developed earlier in Ref. [60] and applied to both linear scattering and absorption and to third-harmonic generation in thin free-electron nanofilms with diffuse boundaries. Here this approach is modified and generalized to spherical free-electron nanoclusters with diffuse surface. As for nanofilms, two different perturbation theories corresponding to different ranges of the laser intensity are developed, and the decisive role of the diffuse surface of the cluster in all of the considered processes is revealed.

The article is organized as follows. Section II contains the statement of the problem of the nonlinear laser-cluster interaction in the hydrodynamic approximation, allowing for fully nonlinear scattering and absorption of the laser field by the cluster. We also present an outline of the corresponding static problem both for cold metal clusters and for hot laser-heated/ionized clusters. In Eq. (7) we define a crucial dimensionless parameter A , whose value (zero or nonzero) determines the type of perturbation theory that one has to employ. For cold and for hot clusters, respectively, the cluster parameter A can be represented as the squared ratio of a quantum length or the Debye screening length over the cluster radius. For $A = 0$, in the static regime complete local compensation of the positive and negative charges takes place in all parts of the cluster. We will hereafter refer to this case as the charge compensation approximation (CCA). The main effect of nonzero A then is a deviation of the static electron density from the ion-charge density near the cluster surface. With the CCA and without the CCA, two different perturbation theories will be developed, which work in different ranges of the laser intensity. Section III contains the general theory of harmonic generation by free-electron nanoclusters due to the nonlinear collective electron motion. Specific results for the basic case of the linear cluster response are presented in Sec. IV. In this article, we restrict ourselves to a detailed investigation of the linear response of the free-electron cluster with diffuse surface. Concrete results for the dynamical problems of *nonlinear* scattering and absorption and, in particular, of THG will be considered in a separate paper. Section IV A is based on the linear cluster response in the CCA (both for neutral and for positively charged clusters), while Sec. IV B goes beyond the CCA (both for neutral cold metal clusters and for hot laser heated/ionized clusters). Concluding remarks terminate the article in Sec. V.

II. HYDRODYNAMIC APPROACH TO THE NONLINEAR LASER-CLUSTER INTERACTION AND THE CLUSTER DIPOLE RESPONSE

We are interested in the dynamics of the electron subsystem of the cluster and will assume that the ion subsystem is frozen on the time scale of the laser-cluster interaction. We will also neglect electron-ion and electron-electron binary collisions in the process of the collective electron motion in the restricted volume of the nanocluster affected by the laser field. Under these conditions, the electron density $n_e(t, \mathbf{r})$, the electron current $\mathbf{q}(t, \mathbf{r}) = n_e \bar{\mathbf{v}}(t, \mathbf{r})$ with $\bar{\mathbf{v}}(t, \mathbf{r})$ the average electron velocity, and the electron pressure tensor $P_{\alpha\beta}(t, \mathbf{r})$ satisfy the

collisionless hydrodynamic equations

$$\frac{\partial n_e}{\partial t} + \text{div } \mathbf{q} = 0, \quad (1a)$$

$$\frac{\partial q_\alpha}{\partial t} + \gamma \omega_p q_\alpha + \frac{\partial (P_{\alpha\beta}/m_e + q_\alpha q_\beta/n_e)}{\partial x_\beta} + \frac{en_e}{m_e} (E_\alpha + E_\alpha^L) + \frac{e}{m_e c} e_{\alpha\beta\gamma} q_\beta (H_\gamma + H_\gamma^L) = 0, \quad (1b)$$

$$\frac{\partial P_{\alpha\beta}}{\partial t} + \frac{1}{n_e} (\mathbf{q} \cdot \nabla) P_{\alpha\beta} + P_{\alpha\gamma} \frac{\partial (q_\beta/n_e)}{\partial x_\gamma} + P_{\beta\gamma} \frac{\partial (q_\alpha/n_e)}{\partial x_\gamma} + P_{\alpha\beta} \text{div} (\mathbf{q}/n_e) + \frac{e}{m_e c} (e_{\alpha\gamma\delta} P_{\beta\gamma} + e_{\beta\gamma\delta} P_{\alpha\gamma}) \times (H_\delta + H_\delta^L) = 0. \quad (1c)$$

In Eqs. (1), m_e is the electron mass, e is the absolute value of the electron charge, c is the speed of light, $\mathbf{E}^L(t, \mathbf{r})$ and $\mathbf{H}^L(t, \mathbf{r})$ are the electric and magnetic components of the external electromagnetic field acting on the cluster, and $\mathbf{E}(t, \mathbf{r})$ and $\mathbf{H}(t, \mathbf{r})$ are the self-consistent electric and magnetic fields of the ions and electrons of the cluster. (Because we consider nonmagnetic clusters in a nonmagnetic medium, the magnetic field and the magnetic induction are always identical.) The tensor $e_{\alpha\beta\gamma}$ denotes the completely antisymmetric Levi-Civita tensor, and summation over repeated indices is always implied. The origin of the coordinate system will always be at the center of the spherical cluster.

Equations (1) describe the collective dynamics of the free electron gas in a nanocluster exposed to the laser field if the nanocluster diameter, for which we assume the range of 1–100 nm, is smaller than the electron mean free path due to binary collisions. However, the collective interaction of the electrons confined within the cluster with the cluster surface is included. Indeed, it is the presence of the electron interaction with the nanocluster surface that allows us to ignore binary collisions and justifies the hydrodynamic approximation in the collisionless regime. The relative weakness of the binary collisions in the nanocluster permits us to omit in Eq. (1c) the dissipative terms with the transport coefficients. Their presence in the conventional hydrodynamic equations is directly connected with the Boltzmann collision integral [61–63]. This is the main approximation of our hydrodynamic model.

Equations (1) can be directly obtained from the collisionless Vlasov kinetic equation for the electron distribution function $f_e(t, \mathbf{r}, \mathbf{p})$ (with nonrelativistic electron momentum $\mathbf{p} = m_e \mathbf{v}$),

$$\frac{\partial f_e}{\partial t} + (\mathbf{v} \cdot \nabla) f_e - e \left\{ (E_\alpha + E_\alpha^L) + e_{\alpha\beta\gamma} \frac{v_\beta}{c} (H_\gamma + H_\gamma^L) \right\} \times \frac{\partial f_e}{\partial p_\alpha} = 0, \quad (2)$$

by integrating Eq. (2) over momentum, respectively, with factors 1, v_α , and $v_\alpha v_\beta$. In this case [62,63], $n_e = \int f_e d^3 p$, $\mathbf{q} \equiv n_e \bar{\mathbf{v}} = \int \mathbf{v} f_e d^3 p$, and $P_{\alpha\beta} = m_e \int (v_\alpha - \bar{v}_\alpha)(v_\beta - \bar{v}_\beta) f_e d^3 p$. The third-order velocity moments that arise in the derivation of Eq. (1c) disappear for the local-equilibrium distribution function, which is established due to the interaction of the electrons with the cluster boundary. Actually, this only requires that the local-equilibrium distribution function be even with respect to inversion of the various components of the relative-velocity

vector $\mathbf{v} - \bar{\mathbf{v}}$ (the central symmetry), without the requirement of total spherical symmetry in velocity space, which may be violated in the presence of the strong linearly polarized laser field. Qualitatively, this situation can be interpreted in terms of different longitudinal and transverse electron temperatures with respect to the direction of the electric-field vector of the applied laser pulse. Then, beyond the local-equilibrium approximation, third-order velocity moments could only result in the dissipative transport terms, which are due to binary collisions [61–63]. These are disregarded in our hydrodynamic model for nanoclusters with the diameters smaller than the binary-collision mean free path.

On the other hand, the second (relaxation) term in Eq. (1b) with the dimensionless relaxation constant γ , which is normalized to the bulk plasma frequency $\omega_p = \sqrt{4\pi e^2 z_i n_{\text{ion}}/m_e}$, was introduced phenomenologically. Here z_i is the mean ionic charge and n_{ion} is the reference bulk ion density of the cluster substance. We include this collisionlike term, which simulates weak binary collisions, because the solution of the hydrodynamic equations (1) even in the collisionless case implies the limit of $\gamma \rightarrow +0$, which may not coincide with the result of direct substitution $\gamma = 0$.

Note that Eqs. (1) form a closed system of equations for the electron density, the mean electron velocity, and all components of the electron pressure tensor. As is usually done in conventional hydrodynamics [61–63], the pressure tensor can be presented in the form $P_{\alpha\beta} = P\delta_{\alpha\beta} + \pi_{\alpha\beta}$, with $P = P_{\alpha\alpha}/3$ the scalar pressure and $\pi_{\alpha\beta}$ the stress tensor ($\pi_{\alpha\alpha} = 0$). In the isotropic case with a spherically symmetric velocity distribution function, $\pi_{\alpha\beta}$ vanishes in the local-equilibrium approximation. It may only reappear beyond the local-equilibrium approximation through the Boltzmann integral as a dissipative term connected with viscosity, as was the case for the third-order moments. However, $\pi_{\alpha\beta}$ may not vanish in the presence of a strong linearly polarized laser field, if the spherical symmetry of the local-equilibrium distribution is reduced to only inversion symmetry. In this case, in contrast to the third-order moments, the *nondissipative* contribution to the stress tensor $\pi_{\alpha\beta}$ may be nonzero in the collisionless case (with respect to the binary collisions) due to the applied laser field. In this case, the actual values of the stress-tensor components, which are induced by the laser field, may only be found self-consistently as a result of solution of Eqs. (1). For this reason, in what follows we do not divide the pressure tensor into two parts as indicated above and do not rewrite Eq. (1c) in a form similar to conventional hydrodynamics but will rather work with the complete pressure tensor $P_{\alpha\beta}$ and the system of Eqs. (1).

The hydrodynamic equations (1) are essentially nonlinear. Perturbation expansions with respect to the incident laser wave [specified by $\mathbf{E}^L(t, \mathbf{r})$ and $\mathbf{H}^L(t, \mathbf{r})$] of the electron density, current, and pressure, as well as the self-consistent electric and magnetic fields, have the form

$$n_e(t, \mathbf{r}) = n_e^{(0)}(r) + 2\text{Re} \sum_{n=1}^{\infty} \sum_{l=0}^n n_e^{(nl)}(t, \mathbf{r}), \quad (3a)$$

$$\mathbf{q}(t, \mathbf{r}) = 2\text{Re} \sum_{n=1}^{\infty} \sum_{l=0}^n \mathbf{q}^{(nl)}(t, \mathbf{r}), \quad (3b)$$

$$P_{\alpha\beta}(t, \mathbf{r}) = \delta_{\alpha\beta} P^{(0)}(r) + 2\text{Re} \sum_{n=1}^{\infty} \sum_{l=0}^n P_{\alpha\beta}^{(nl)}(t, \mathbf{r}), \quad (3c)$$

$$\mathbf{E}(t, \mathbf{r}) = \mathbf{E}^{(0)}(r) + 2\text{Re} \sum_{n=1}^{\infty} \sum_{l=0}^n \mathbf{E}^{(nl)}(t, \mathbf{r}), \quad (3d)$$

$$\mathbf{H}(t, \mathbf{r}) = 2\text{Re} \sum_{n=1}^{\infty} \sum_{l=0}^n \mathbf{H}^{(nl)}(t, \mathbf{r}), \quad (3e)$$

where the index n denotes the order of nonlinearity with respect to the incident field. For a monochromatic external field, each n th-order term can be Fourier expanded. The corresponding summation index is denoted by l , where, of course, $0 \leq l \leq n$ for the n th-order term. Hence, we have $n_e^{(nl)}(t, \mathbf{r}) = n_e^{(nl)}(\mathbf{r}) e^{-i(n-l)\omega t}$, $\mathbf{q}^{(nl)}(t, \mathbf{r}) = \mathbf{q}^{(nl)}(\mathbf{r}) e^{-i(n-l)\omega t}$, $P_{\alpha\beta}^{(nl)}(t, \mathbf{r}) = P_{\alpha\beta}^{(nl)}(\mathbf{r}) e^{-i(n-l)\omega t}$, $\mathbf{E}^{(nl)}(t, \mathbf{r}) = \mathbf{E}^{(nl)}(\mathbf{r}) e^{-i(n-l)\omega t}$, and $\mathbf{H}^{(nl)}(t, \mathbf{r}) = \mathbf{H}^{(nl)}(\mathbf{r}) e^{-i(n-l)\omega t}$. In Eq. (3c) and hereafter, $\delta_{\alpha\beta}$ is the Kronecker symbol. For the order n of nonlinearity in the laser field, the n th-order harmonic frequency $n\omega$ corresponds to the amplitudes with $l = 0$, but the n th-order amplitudes with nonzero $l \leq n$ corresponding to lower frequencies can also be present in Eqs. (3). Note that some of these amplitudes with particular l may identically vanish, and all the nonvanishing amplitudes should be found from the total set of nonlinear hydrodynamic equations (1) and the linear Maxwell equations

$$\text{div } \mathbf{E} = 4\pi e(z_i n_i - n_e), \quad \text{div } \mathbf{H} = 0, \quad (4a)$$

$$\text{rot } \mathbf{E} = -\frac{1}{c} \frac{\partial \mathbf{H}}{\partial t}, \quad \text{rot } \mathbf{H} = \frac{1}{c} \frac{\partial \mathbf{E}}{\partial t} - \frac{4\pi e \mathbf{q}}{c}. \quad (4b)$$

In Eqs. (4), $n_i(r)$ is the spherically symmetric spatial density of the positive ions in the cluster with diffuse surface. The electron density, pressure, and self-consistent electric field $\mathbf{E}(t, \mathbf{r})$ in Eqs. (3) are divided into two parts, namely the zeroth-order static contributions $n_e^{(0)}(r)$, $\delta_{\alpha\beta} P^{(0)}(r)$, and $\mathbf{E}^{(0)}(r)$, which exist before the action of the laser field, and the contributions induced by the external laser field, which in a nonlinear medium formally include all orders $n = 1, 2, \dots, \infty$ of the perturbation expansion with respect to the laser field. The electron current as well as the self-consistent magnetic field $\mathbf{H}(t, \mathbf{r})$ vanish in the initial equilibrium without the laser field, and the condition $n = 1$ in all these quantities corresponds to the linear approximation with respect to the laser field. Only the first (electrostatic) Maxwell equation should be used in the corresponding zeroth-order static (quasi-equilibrium) problem, prior to the action of the laser pulse (or prior to the action of the probe pulse in the case of a nanocluster laser-heated/ionized by strong pump wave).

For the spherically symmetric cluster that we consider, a jellium model ion density with diffuse surface can be presented as $n_i(r) = n_{\text{ion}}$ for $r - R \leq -\sigma/2$, $n_i(r) = 0$ for $r - R \geq \sigma/2$, and $n_i(r) = n_{\text{ion}} g((r - R)/\sigma)$ for $|r - R| < \sigma/2$, where R is the cluster radius. The parameter σ characterizes the small diffuseness of the cluster surface (it is implied that the condition $\sigma \ll R$ is always met). The dimensionless function $g(x)$ specifies the profile [with the dimensionless argument $x = (r - R)/\sigma$, $|x| < 1/2$] of the ion density in the diffuse cluster surface. Over the distance σ , it drops

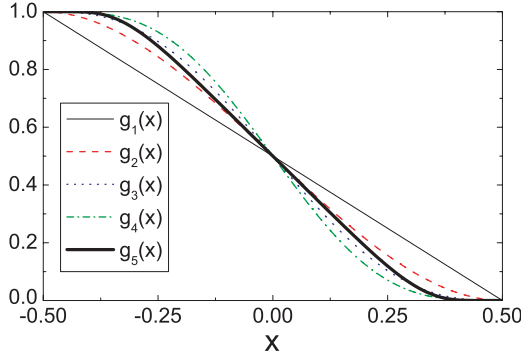


FIG. 1. (Color online) The model profiles of the diffuse surface $g_i(x)$ with different smoothness ($i = 1 - 5$, see text) for spherical clusters, with $x = (r - R)/\sigma$.

in our model from its reference bulk value n_{ion} to zero. If $\sigma = 0$, then $n_i(r) = 0$ for $r > R$ and $n_i(r) = n_{\text{ion}}$ for $r \leq R$ (the steplike ion density). For $\sigma \neq 0$, the simplest continuous trapezoidal profile $g(x) \equiv g_1(x) = -x + 0.5$ can be used to model the ion background inside the diffuse cluster surface. Alternatively, as shown in Fig. 1, different polynomial profiles can be used with smoother behavior at $x = \pm 1/2$: $g(x) \equiv g_2(x) = 2x^3 - 1.5x + 0.5$ (with continuous first derivative), $g(x) \equiv g_3(x) = -6x^5 + 5x^3 - 1.875x + 0.5$ (with continuous second derivative), $g(x) \equiv g_4(x) = 20x^7 - 21x^5 + 8.75x^3 - 2.1875x + 0.5$ (with continuous third derivative), or $g(x) \equiv g_5(x) = (1 - \tanh(\tan(\pi x)))/2$ (a completely smooth profile). To avoid the edge singularities in the following calculations, using the completely smooth profile is most preferable.

Before considering the dynamical problem, let us discuss the equilibrium cluster state without the laser field. In this case, Eqs. (1), (3), and (4) result in two equations for the zeroth-order static functions $n_e^{(0)}(r)$, $P^{(0)}(r)$, and $E^{(0)}(r)$ (the latter is defined from $E^{(0)}(r) \equiv E^{(0)}(r)\mathbf{n}$, with $\mathbf{n} = \mathbf{r}/r$ the unit radius vector):

$$\frac{dP^{(0)}}{dr} + en_e^{(0)}E^{(0)} = 0, \quad \frac{1}{r^2} \frac{d(r^2 E^{(0)})}{dr} = 4\pi e(z_i n_i - n_e^{(0)}). \quad (5)$$

These equations should be complemented by the equation of state of the electron gas, which relates the equilibrium electron pressure, the equilibrium electron density, and the gas temperature. For metal clusters at room temperature, the zero-temperature approximation can be used with good accuracy, and the relation between the electron pressure and the electron density can be taken from the Thomas-Fermi model as $P^{(0)} = \frac{2}{5}n_e^{(0)}\varepsilon_F(n_e^{(0)})$, with the local Fermi energy $\varepsilon_F(n_e^{(0)}) = (3\pi^2)^{2/3}\hbar^2(n_e^{(0)})^{2/3}/(2m_e)$. Equations (5) can be rewritten in dimensionless form by introducing the dimensionless radial variable $\rho = r/R$, the dimensionless equilibrium electron density $n_0(\rho) = n_e^{(0)}(r)/(z_i n_{\text{ion}})$ (with respect to the bulk electron density), the dimensionless equilibrium electron pressure $p_0(\rho) = P^{(0)}(r)/P_0$, with the electron bulk pressure $P_0 = \frac{2}{5}z_i n_{\text{ion}}\varepsilon_F(z_i n_{\text{ion}})$, the dimensionless static electric field $\mathcal{E}_0(\rho) = E^{(0)}(r)/(4\pi e z_i n_{\text{ion}} R)$ (with $\mathcal{E}_0(\rho) = E_0(\rho)\mathbf{n}$), and the dimensionless ion-density profile $\Theta_i(\rho) = n_i(r)/n_{\text{ion}}$. With

these notations, Eqs. (5) take the form

$$A \frac{dp_0}{d\rho} + n_0 \mathcal{E}_0 = 0, \quad \frac{d\mathcal{E}_0}{d\rho} + \frac{2\mathcal{E}_0}{\rho} = \Theta_i(\rho) - n_0, \quad (6)$$

with the dimensionless equation of state $p_0 = n_0^{5/3}$ for cold metal clusters.

The dimensionless parameter A , which occurs in Eq. (6), is generally defined as

$$A = \frac{P_0}{4\pi e^2 z_i^2 n_{\text{ion}}^2 R^2}. \quad (7)$$

For the current case of cold metal clusters it can be presented as $A = (l_Q/R)^2$, with $l_Q = 3^{1/3}\pi^{1/6}\hbar/[e\sqrt{20m_e}(z_i n_{\text{ion}})^{1/6}]$. Typical values of the quantum length l_Q are in the range of 0.01 – 0.1 nm. This is smaller than even the minimal surface diffuseness, which is of the order of the interatomic distance in metals (about 0.3 nm). It is much smaller than the nanocluster radius, which typically is of the order of $R \sim 10$ nm. Hence, the parameter A is very small indeed, about $A \sim 10^{-5}$. A similar situation occurs for the case of hot clusters heated by a pump laser prepulse to a temperature T that exceeds the Fermi temperature, so that classical Boltzmann statistics are applicable. For such laser-heated clusters the equation of state is $P(0) = n_e^{(0)}T$. If we set $P_0 = z_i n_{\text{ion}}T$, we again obtain the dimensionless Eqs. (6), but now with the dimensionless equation of state $p_0 = n_0$ for hot laser-heated clusters. In this case, the parameter A can be written as $A = (l_D/R)^2$, with $l_D = \sqrt{T/(4\pi e^2 z_i n_{\text{ion}})}$ the conventional Debye screening length. Again, values of the parameter A are typically small. Typical values of the Debye length for a cluster at a temperature $T \sim 100$ eV (and still with the reference bulk electron density) are in the range of 0.1 – 1 nm, so for clusters with radius $R \sim 10$ nm we have $A \sim 10^{-3}$. However, the parameter A increases with decreasing ion density (e.g., due to expansion of the hot laser-heated cluster).

In view of the above, to a first approximation the parameter A can be set equal to zero. In the case of $A = 0$, regardless of the equation of state, Eqs. (6) have the obvious solution $n_0(\rho) = \Theta_i(\rho)$, $\mathcal{E}_0(\rho) = 0$, if we consider neutral clusters (either cold metal clusters or hot laser-heated clusters). This means that in this case exact local compensation of positive and negative charges occurs throughout the whole cluster volume. For diffuse (but not for steplike) cluster surface, deviation of the parameter A from zero leads to violation of the local compensation of the negative charge of the electrons and the positive charge of the ion background at least in the narrow range of the cluster surface and to creation of a charged double layer. (For a steplike cluster surface, violation of the local compensation of the positive and negative charges near the surface and spill-out of the electrons outside the cluster surface can only occur due to quantum-mechanical effects, including the metal work function and tunneling, which are not taken into account in this work.) For this reason, the case of $A = 0$ is referred to hereafter as the CCA (the charge compensation approximation). Note that the CCA is formally equivalent to the approximation of a cold plasma, which is widely used in conventional plasma physics [61–63], because the condition $\sqrt{A} \ll 1$ can be rewritten in the form of $v_T \ll R\omega_p$ or $v_F \ll R\omega_p$ for hot or cold clusters, respectively, with v_T and v_F the thermal or the Fermi velocity of the electrons.

However, unlike the common case of an extended plasma, whether the plasma can be considered as cold depends on the cluster radius (see the right-hand side of conditions above). In the context of our study, the interpretation of the case $A = 0$ as the CCA seems more relevant for the confined plasma of nanoclusters. Also, deviation of the parameter A from zero results in the appearance of a static electric field in the cluster-surface region, which traps the electrons in the cluster. For a cold metal cluster, this electric field is of the order of $4\pi e z_i n_{\text{ion}} l_Q \sim 10^8$ V/cm. In spite of the smallness of A , its influence may be important for those processes, for which the cluster surface plays a decisive role (e.g., for third-harmonic generation [36,37,60]).

Formally, in the case of neutral clusters the solution of Eqs. (6) with $A \neq 0$ may be extended to the region outside the cluster boundary $\rho = 1 + \sigma/(2R)$, which results in an electron halo around the cluster. Even without the quantum spill-out effect mentioned above, this situation could be realized in our model for clusters with diffuse surface in vacuum. However, it is unlikely for a cold neutral metal cluster embedded into a surrounding nonconducting bulk medium such as a transparent dielectric. Assuming the latter case, we rule out the presence of an electron halo by making sure that the electron density vanishes everywhere at $\rho > 1 + \sigma/(2R)$, that is, outside the exterior of the diffuse cluster surface. In some cases the cluster may be positively charged. Especially, this may be the case for hot laser-heated clusters in vacuum, when electrons actually have escaped from the cluster during the interaction of the cluster with the strong pump laser pulse. For the subsequent interaction of the charged cluster with the probe laser pulse, an outer-ionization degree η defined as

$$\eta = 1 - \int_0^{\rho_{\text{lim}}} n_0(\rho) \rho^2 d\rho \Big/ \int_0^{1+\sigma/(2R)} \Theta_i(\rho) \rho^2 d\rho \quad (8)$$

will take into account the global lack of compensation of the positive and negative charges of the cluster. Here, allowing for the possible presence of an electron halo outside the cluster surface, we have introduced a limiting radius of integration $\rho_{\text{lim}} \geq 1 + \sigma/(2R)$, beyond which the electron density vanishes. The boundary condition

$$\mathcal{E}_0(\rho = \rho_{\text{lim}}) = \eta \int_0^{1+\sigma/(2R)} \Theta_i(\rho) \rho^2 d\rho \Big/ \rho_{\text{lim}}^2 \quad (9)$$

should then be imposed on the solutions of Eqs. (6) at this upper limit $\rho = \rho_{\text{lim}}$. Note that in the CCA, that is in the approximation of $A = 0$, the solution of Eqs. (6) for a positively charged cluster results in local compensation of the positive and negative charges in the central part of the cluster as far as possible (with a sharp boundary at some radius R_c), while leaving the rest (near-surface) zone of the cluster completely without electrons. Of course, the latter zone is generally unstable and is affected by Coulomb explosion. The radius R_c of the globally neutral core of the charged cluster with given outer-ionization degree η is defined by the condition

$$\eta = 1 - \int_0^{R_c/R} \Theta_i(\rho) \rho^2 d\rho \Big/ \int_0^{1+\sigma/(2R)} \Theta_i(\rho) \rho^2 d\rho. \quad (10)$$

Hence, for $A = 0$, we have $n_0(\rho) = \Theta_i(\rho)$ and therefore $\mathcal{E}_0(\rho) = 0$ for $\rho \leq R_c/R$, while $n_0(\rho) = 0$ and

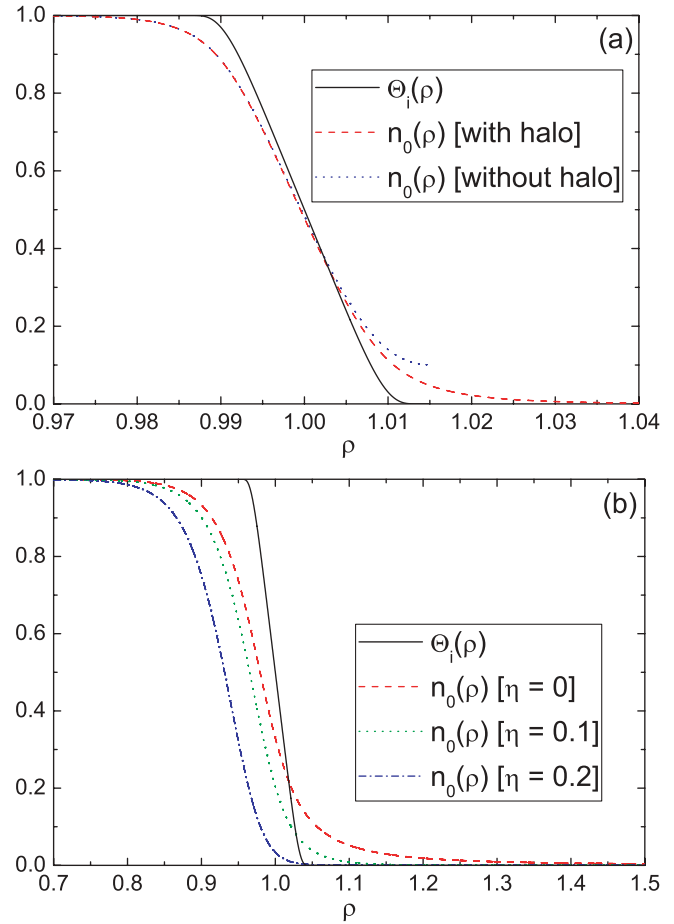


FIG. 2. (Color online) The electron density $n_0(\rho)$ near the cluster surface as a result of solution of Eqs. (6) for cold neutral metal clusters in vacuum [with a halo] and in a surrounding dielectric matrix [without halo] (a) and hot laser heated/ionized clusters in vacuum (b). For (a) $A = 10^{-5}$, $\sigma/R = 3 \times 10^{-2}$. For (b) $A = 10^{-3}$, $\sigma/R = 10^{-1}$, $\eta = 0, 0.1$, and 0.2 . For the ion density of the cluster surface region, the completely smooth profile $g_5(x)$ is used (see Fig. 1).

$\mathcal{E}_0(\rho) = [\int_{R_c/R}^{\rho} \Theta_i(\rho) \rho^2 d\rho] / \rho^2$ for $R_c/R < \rho < 1 + \sigma/(2R)$. Nonzero A results in a diffuse transition range from the inner neutral core to the positively charged shell. In Fig. 2, examples of a numerical solution of Eqs. (6) at $A \neq 0$ both for cold neutral metal clusters (without and with the electron halo, for comparison) and for hot laser heated/ionized clusters are presented.

For completeness, a well-known fact [64] should be noted here: for hot clusters with classical Boltzmann statistics of the electrons, in equilibrium a residual nonzero electron density should exist, in principle, everywhere outside the cluster. This is because the static Eqs. (6) together with $p_0 = n_0$ and $\mathcal{E}_0 = -\partial\varphi_0/\partial\rho$ (where $\varphi_0(\rho)$ is the dimensionless static electric potential) yield $n_0(\rho) = n_0(0) \exp\{[\varphi_0(\rho) - \varphi_0(0)]/A\}$. If we choose, as it is natural, that $\varphi_0(\rho) \rightarrow 0$ at $\rho \rightarrow \infty$, then $n_0(\rho) \rightarrow n_0(0) \exp(-\varphi_0(0)/A) \equiv n_0(0) \exp[-\varphi_0(0)(R/l_D)^2]$ at $\rho \rightarrow \infty$. Because the dimensionless static electric potential $\varphi_0(0) = -\int_{\infty}^0 \mathcal{E}_0(\rho) d\rho$ is approximately $10A$ (the coefficient was estimated numerically), this residual constant electron density is relatively very small and does not play any role for nanoclusters under the conditions considered. The negligibility

of the relative residual electron density was also justified by our numerical solutions of Eqs. (6) for hot laser-heated nanoclusters for all the cluster parameters used. On the other hand, the electron halo in the immediate vicinity of the cluster surface may be appreciable, especially for neutral clusters.

For the dynamical problem, we will assume an incident linearly polarized plane electromagnetic wave that propagates in the positive x direction and has its electric-field vector in the z direction, so that

$$\mathbf{E}^{(\text{in})}(t, \mathbf{r}) = 2\text{Re}\{E_0 \mathbf{e}_z e^{i\mathbf{k}_1 \cdot \mathbf{r} - i\omega t}\}, \quad (11a)$$

$$\mathbf{H}^{(\text{in})}(t, \mathbf{r}) = \frac{c}{\omega} [\mathbf{k}_1 \times \mathbf{E}^{(\text{in})}], \quad (11b)$$

where E_0 is the complex amplitude of the laser electric field with intensity $I_0 = \sqrt{\epsilon_1} c |E_0|^2 / (2\pi)$, ω the laser frequency, $\mathbf{k}_1 = k_1 \mathbf{e}_x$ the fundamental wave vector with $k_1 = \sqrt{\epsilon_1} \omega / c$, and \mathbf{e}_x and \mathbf{e}_z are Cartesian unit vectors. We have assumed that the cluster is surrounded by a transparent nonmagnetic dielectric medium with real dielectric permittivities $\epsilon_n \equiv \epsilon(n\omega)$ for different harmonics and that E_0 is the electric field amplitude of the incident laser wave in the dielectric. The dielectric surroundings may be especially of interest for cold metal clusters. In this case, the amplitude E_L of the external field inside the cluster, which should be considered as the electric field in a small spherical hole in the dielectric, is connected with the corresponding electric-field amplitude E_0 of the laser wave by the condition $E_L = (2 + \epsilon_1) E_0 / 3$ [65]. The electric and magnetic fields $\mathbf{E}^L(t, \mathbf{r})$ and $\mathbf{H}^L(t, \mathbf{r})$, which enter Eqs. (1b) and (1c) and act as external fields on the cluster electrons, are

$$\mathbf{E}^L(t, \mathbf{r}) = \frac{2 + \epsilon_1}{3} \mathbf{E}^{(\text{in})}(t, \mathbf{r}) = 2\text{Re}\{E_L \mathbf{e}_z e^{i\mathbf{k}_1 \cdot \mathbf{r} - i\omega t}\}, \quad (12a)$$

$$\mathbf{H}^L(t, \mathbf{r}) \equiv \mathbf{H}^{(\text{in})}(t, \mathbf{r}) = \frac{c}{\omega} [\mathbf{k}_1 \times \mathbf{E}^{(\text{in})}]. \quad (12b)$$

Solutions of the Maxwell equations (4) should be given separately in the range $0 < r/R < \rho_{\text{lim}}$ (inside the cluster including its diffuse surface and including the electron halo, if necessary, where free electrons are present) and in the outside range $r/R > \rho_{\text{lim}}$ [in the surrounding dielectric medium for cold metal clusters with $\rho_{\text{lim}} = 1 + \sigma/(2R)$ or in the vacuum outside the electron halo both for cold metal clusters and for hot laser-heated/ionized clusters], where the first and the last equations from Eqs. (4) for the n th-order nonlinear terms should be replaced, respectively, by $\text{div } \mathbf{E}^{(nl)} = 0$ and $\text{rot } \mathbf{H}^{(nl)} = \{i\epsilon_{n-1}(n-l)\omega/c\} \mathbf{E}$. In the outer range, the self-consistent electromagnetic field coincides with the scattered radiation both at the fundamental laser frequency and at the harmonic frequencies, which are generated due to the cluster's hydrodynamical nonlinearities. In the following, we restrict ourselves to the dipole approximation. This requires that the inequality $k_n R \ll 1$ for the order n of nonlinearity (with $k_n = \sqrt{\epsilon_n} n\omega/c$) be satisfied. This is the case for the small nanoclusters that we consider and, at least, for infrared fundamental laser radiation and harmonics of moderate order. We should also restrict ourselves to the nonrelativistic case, when the typical electron velocity (either the Fermi velocity in the case of cold metal nanoclusters or the thermal velocity for hot laser-heated/ionized nanoclusters) is small compared with the speed of light. In the dipole approximation, both the radiation and the absorption of the free-electron nanocluster

are determined by the time-dependent electric dipole moment

$$\mathbf{d}(t) = -e \int \mathbf{r} n_e d^3 r = 2\text{Re} \sum_{n=1}^{\infty} \sum_{l=0}^n \mathbf{d}^{(nl)}(t). \quad (13)$$

The quantity $\mathbf{d}^{(nl)}(t) = -e \int \mathbf{r} n_e^{(nl)} d^3 r \sim e^{-i(n-l)\omega t}$ denotes the n th-order dipole moment for particular l , which is nonlinearly induced by the electric component of the external electromagnetic field at the cluster center, that is, by the field $\mathbf{E}^L(t) \equiv \mathbf{E}^L(t, \mathbf{r} = 0) = 2\text{Re}\{E_L \mathbf{e}_z e^{-i\omega t}\} \equiv 2\text{Re} \mathbf{E}^{\text{cL}}(t)$. The external magnetic field at the cluster center is $\mathbf{H}^L(t) \equiv \mathbf{H}^L(t, \mathbf{r} = 0) = 2\text{Re}\{(c/\omega)[\mathbf{k}_1 \times E_0 \mathbf{e}_z] e^{-i\omega t}\} \equiv 2\text{Re} \mathbf{H}^{\text{cL}}(t)$. Here $\mathbf{E}^{\text{cL}}(t) = E_L \mathbf{e}_z e^{-i\omega t}$ and $\mathbf{H}^{\text{cL}}(t) = -\sqrt{\epsilon_1} E_0 \mathbf{e}_y e^{-i\omega t}$ are the corresponding complex external electric and magnetic fields. For the order n of nonlinearity, for free-electron nanoclusters the scattered radiation at the frequency $n\omega$ is mainly determined by the corresponding time-dependent electric dipole moment of the cluster $\mathbf{d}^{(n0)}(t) \sim e^{-in\omega t}$ (if it is not identically zero due to symmetry, as is the case for even harmonics for spherical clusters, for which higher multipoles should be taken into account). The term $\mathbf{d}^{(nn-1)}(t) \sim e^{-i\omega t}$ in Eq. (13) is responsible for the nonlinear corrections (at $n > 1$) to linear absorption (at $n = 1$) at the fundamental laser frequency, so the mean power Q absorbed by the cluster is generally expressed as

$$Q = \sum_{n=1}^{\infty} Q_n = 2\omega \text{Im} \sum_{n=1}^{\infty} \mathbf{d}^{(nn-1)} \cdot (\mathbf{E}^{\text{cL}})^*. \quad (14)$$

Let us turn to a solution of the Maxwell equations in the range $r/R > \rho_{\text{lim}}$ outside the cluster and the possible electron halo. The scattered electric field at the harmonic order n can be presented as

$$\mathbf{E}^{(n0)}(t, \mathbf{r}) = \text{rot} \{g^{(n0)}(r) [\mathbf{n} \times \mathbf{d}^{(n0)}(t)]\}, \quad (15)$$

with $g^{(n0)}(r) = ik_n [1 + i(k_n r)^{-1}] e^{ik_n r} / (\epsilon_n r)$. The corresponding magnetic field is $\mathbf{H}^{(n0)}(t, \mathbf{r}) = \sqrt{\epsilon_n} (ik_n)^{-1} \text{rot } \mathbf{E}^{(n0)}(t, \mathbf{r})$. At large distances satisfying the condition $k_n r \gg 1$ the scattered electric field is

$$\mathbf{E}^{(n0)}(t, \mathbf{r}) = \frac{k_n^2}{\epsilon_n} [\mathbf{d}^{(n0)} - \mathbf{n}(\mathbf{n} \cdot \mathbf{d}^{(n0)})] \frac{e^{ik_n r}}{r}, \quad (16)$$

with $\mathbf{H}^{(n0)}(t, \mathbf{r}) = \sqrt{\epsilon_n} [\mathbf{n} \times \mathbf{E}^{(n0)}(t, \mathbf{r})]$, while on the halo limiting boundary $\mathbf{r} = R\rho_{\text{lim}} \mathbf{n}$ near the cluster surface, provided that $k_n r \ll 1$, we obviously obtain

$$\mathbf{E}^{(n0)}(t, \mathbf{r} = R\rho_{\text{lim}} \mathbf{n}) = \frac{3\mathbf{n}(\mathbf{n} \cdot \mathbf{d}^{(n0)}) - \mathbf{d}^{(n0)}}{\epsilon_n (R\rho_{\text{lim}})^3}. \quad (17)$$

With our definitions, the intensity I_n of the dipole radiation scattered at the n th-order harmonic frequency $n\omega$ is given by the expression

$$I_n = \frac{4(n\omega)^4 \sqrt{\epsilon_n}}{3c^3} |\mathbf{d}^{(n0)}|^2. \quad (18)$$

Note that this is only the main contribution to the harmonic intensity at the frequency $n\omega$, because corrections to this expression arise from orders of nonlinearity higher than n (with $l \neq 0$). Assuming that the perturbation expansion converges sufficiently fast, we will neglect these corrections. The nonvanishing electric dipole moment of the cluster $\mathbf{d}^{(n0)}(t)$, which determines the intensity of generation of the

n th-order harmonic by the cluster, can be found through the corresponding electron density contribution $n_e^{(n)}(t, \mathbf{r})$. The latter can be determined by solving the corresponding inner dynamical problem for the cluster electrons.

III. HARMONIC GENERATION BY THE COLLECTIVE ELECTRON MOTION IN A CLUSTER: THE GENERAL FORMALISM

By substituting Eqs. (3) into Eqs. (1) and collecting both the same order of nonlinearity n and the same time dependence

$e^{-i(n-l)\omega t}$, a set of equations for the amplitudes with different n and l can be obtained. The amplitudes with $l = 0$ form a closed system of equations, which is independent of the amplitudes with $l \neq 0$. On the other hand, the equations for the amplitudes $l \neq 0$ contain the amplitudes with $l = 0$ as source terms. These amplitudes describe higher-order corrections to the main nonlinear contributions and, in particular, nonlinear absorption of the fundamental wave. The system of equations for the amplitudes with $l = 0$ and with $n \geq 1$, which describe n th-order harmonic generation, is

$$-in\omega n_e^{(n)} + \text{div } \mathbf{q}^{(n)} = 0, \quad (19a)$$

$$\begin{aligned} & \sum_{m_1=0}^n \sum_{m_2=0}^{n-m_1} \left\{ (-im_1\omega + \gamma\omega_p) q_\alpha^{(m_1)} n_e^{(m_2)} n_e^{([n-m_1-m_2]0)} + n_e^{([n-m_1-m_2]0)} \left(\frac{n_e^{(m_2)} \partial P_{\alpha\beta}^{(m_1)}}{m_e \partial x_\beta} + \frac{\partial (q_\alpha^{(m_1)} q_\beta^{(m_2)})}{\partial x_\beta} \right) \right. \\ & \left. - q_\alpha^{(m_1)} q_\beta^{(m_2)} \frac{\partial n_e^{([n-m_1-m_2]0)}}{\partial x_\beta} \right\} + \sum_{m_1=0}^n \sum_{m_2=0}^{n-m_1} \sum_{m_3=0}^{n-m_1-m_2} \left\{ \frac{e}{m_e} (E_\alpha^{(m_1)} + \delta_{1m_1} E_\alpha^{cL}) n_e^{(m_2)} n_e^{(m_3)} n_e^{([n-m_1-m_2-m_3]0)} \right. \\ & \left. + \frac{e}{m_e c} e_{\alpha\beta\gamma} q_\beta^{(m_1)} (H_\gamma^{(m_2)} + \delta_{1m_2} H_\gamma^{cL}) n_e^{(m_3)} n_e^{([n-m_1-m_2-m_3]0)} \right\} = 0, \quad (19b) \end{aligned}$$

$$\begin{aligned} & \sum_{m_1=0}^n \sum_{m_2=0}^{n-m_1} \left\{ -im_1\omega P_{\alpha\beta}^{(m_1)} n_e^{(m_2)} n_e^{([n-m_1-m_2]0)} + n_e^{([n-m_1-m_2]0)} \left(q_\gamma^{(m_1)} \frac{\partial P_{\alpha\beta}^{(m_2)}}{\partial x_\gamma} + P_{\alpha\gamma}^{(m_1)} \frac{\partial q_\beta^{(m_2)}}{\partial x_\gamma} \right. \right. \\ & \left. \left. + P_{\beta\gamma}^{(m_1)} \frac{\partial q_\alpha^{(m_2)}}{\partial x_\gamma} + P_{\alpha\beta}^{(m_1)} \frac{\partial q_\gamma^{(m_2)}}{\partial x_\gamma} \right) - \frac{\partial n_e^{([n-m_1-m_2]0)}}{\partial x_\gamma} (P_{\alpha\gamma}^{(m_1)} q_\beta^{(m_2)} + P_{\beta\gamma}^{(m_1)} q_\alpha^{(m_2)} + P_{\alpha\beta}^{(m_1)} q_\gamma^{(m_2)}) \right\} \\ & + \sum_{m_1=0}^n \sum_{m_2=0}^{n-m_1} \sum_{m_3=0}^{n-m_1-m_2} \frac{e}{m_e c} (e_{\alpha\gamma\delta} P_{\beta\gamma}^{(m_1)} + e_{\beta\gamma\delta} P_{\alpha\gamma}^{(m_1)}) (H_\delta^{(m_2)} + \delta_{1m_2} H_\delta^{cL}) n_e^{(m_3)} n_e^{([n-m_1-m_2-m_3]0)} = 0. \quad (19c) \end{aligned}$$

The linear electromagnetic equations inside the cluster are

$$\text{div } \mathbf{E}^{(n)} = -4\pi e n_e^{(n)}, \quad \text{rot } \mathbf{E}^{(n)} = \frac{i n \omega}{c} \mathbf{H}^{(n)}, \quad (20a)$$

$$\text{div } \mathbf{H}^{(n)} = 0, \quad \text{rot } \mathbf{H}^{(n)} = -\frac{i n \omega}{c} \mathbf{E}^{(n)} - \frac{4\pi e \mathbf{q}^{(n)}}{c}. \quad (20b)$$

As for the static equations, Eqs. (19) and (20) can be rewritten in convenient dimensionless form by introducing new dimensionless variables, namely $\boldsymbol{\rho} = \mathbf{r}/R$,

$n_n = n_e^{(n)} / (z_i n_{\text{ion}})$, $p_{n\alpha\beta} = P_{\alpha\beta}^{(n)} / P_0$, $\mathbf{v}_n = \mathbf{v}^{(n)} / (\omega R)$, and $\mathbf{q}_n = \mathbf{q}^{(n)} / (z_i n_{\text{ion}} \omega R)$, as well as $\mathcal{E}_n = \mathbf{E}^{(n)} / (4\pi e z_i n_{\text{ion}} R)$ and $\mathcal{H}_n = \mathbf{H}^{(n)} / (4\pi e z_i n_{\text{ion}} R)$. The same can be done with the external electric and magnetic fields: $\mathcal{E}^L(t) \equiv \mathcal{E}_L \mathbf{e}_z e^{-i\omega t} = \mathbf{E}^{cL}(t) / (4\pi e z_i n_{\text{ion}} R)$, $\mathcal{H}^L(t) \equiv -\mathcal{H}_L \mathbf{e}_y e^{-i\omega t} = \mathbf{H}^{cL}(t) / (4\pi e z_i n_{\text{ion}} R)$, with $\mathcal{E}_L = E_L / (4\pi e z_i n_{\text{ion}} R)$ and $\mathcal{H}_L = \sqrt{\epsilon_1} E_0 / (4\pi e z_i n_{\text{ion}} R)$. In this way, from Eqs. (19) we obtain the following dimensionless inhomogeneous linear equations for the n th-order contributions:

$$-inn_n + \text{div } \mathbf{q}_n = 0, \quad (21a)$$

$$n_0^2 \left\{ \left(-in + \frac{\gamma}{\tilde{\omega}} \right) q_{n\alpha} + \frac{A}{\tilde{\omega}^2} \frac{\partial p_{n\alpha\beta}}{\partial \rho_\beta} + \frac{n_0 (\mathcal{E}_{n\alpha} + \delta_{1n} \mathcal{E}_\alpha^L) + n_n \mathcal{E}_{0\alpha}}{\tilde{\omega}^2} \right\} = V_{n\alpha}, \quad (21b)$$

$$-inn_0^2 p_{n\alpha\beta} + n_0 \frac{\partial p_0}{\partial \rho_\gamma} q_{n\gamma} \delta_{\alpha\beta} + n_0 p_0 \left(\frac{\partial q_{n\beta}}{\partial \rho_\alpha} + \frac{\partial q_{n\alpha}}{\partial \rho_\beta} + \frac{\partial q_{n\gamma}}{\partial \rho_\gamma} \delta_{\alpha\beta} \right) - p_0 \left(q_{n\beta} \frac{\partial n_0}{\partial \rho_\alpha} + q_{n\alpha} \frac{\partial n_0}{\partial \rho_\beta} + q_{n\gamma} \frac{\partial n_0}{\partial \rho_\gamma} \delta_{\alpha\beta} \right) = T_{n\alpha\beta}, \quad (21c)$$

with the right-hand-side source terms

$$\begin{aligned} V_{n\alpha} = & - \sum_{m_1=0}^n \sum_{m_2=0}^{n-m_1} \left\{ \left(-im_1 + \frac{\gamma}{\tilde{\omega}} \right) q_{m_1\alpha} n_{m_2} n_{n-m_1-m_2} + n_{n-m_1-m_2} \left(\frac{A n_{m_2}}{\tilde{\omega}^2} \frac{\partial p_{m_1\alpha\beta}}{\partial \rho_\beta} + \frac{\partial (q_{m_1\alpha} q_{m_2\beta})}{\partial \rho_\beta} \right) - q_{m_1\alpha} q_{m_2\beta} \frac{\partial n_{n-m_1-m_2}}{\partial \rho_\beta} \right\} \\ & - \sum_{m_1=0}^n \sum_{m_2=0}^{n-m_1} \sum_{m_3=0}^{n-m_1-m_2} \left\{ \frac{(\mathcal{E}_{m_1\alpha} + \delta_{1m_1} \mathcal{E}_\alpha^L)}{\tilde{\omega}^2} n_{m_2} n_{m_3} n_{n-m_1-m_2-m_3} + \frac{\tilde{R}}{\tilde{\omega}} e_{\alpha\beta\gamma} q_{m_1\beta} (\mathcal{H}_{m_2\gamma} + \delta_{1m_2} \mathcal{H}_\gamma^L) n_{m_3} n_{n-m_1-m_2-m_3} \right\} \quad (22) \end{aligned}$$

and

$$\begin{aligned}
T_{n\alpha\beta} = & - \sum_{m_1=0}^n \sum_{m_2=0}^{n-m_1} \left\{ -im_1 p_{m_1\alpha\beta} n_{m_2} n_{n-m_1-m_2} + n_{n-m_1-m_2} \left(q_{m_1\gamma} \frac{\partial p_{m_2\alpha\beta}}{\partial \rho_\gamma} + p_{m_1\alpha\gamma} \frac{\partial q_{m_2\beta}}{\partial \rho_\gamma} + p_{m_1\beta\gamma} \frac{\partial q_{m_2\alpha}}{\partial \rho_\gamma} + p_{m_1\alpha\beta} \frac{\partial q_{m_2\gamma}}{\partial \rho_\gamma} \right) \right. \\
& \left. - \frac{\partial n_{n-m_1-m_2}}{\partial \rho_\gamma} (p_{m_1\alpha\gamma} q_{m_2\beta} + p_{m_1\beta\gamma} q_{m_2\alpha} + p_{m_1\alpha\beta} q_{m_2\gamma}) \right\} - \sum_{m_1=0}^n \sum_{m_2=0}^{n-m_1} \sum_{m_3=0}^{n-m_1-m_2} \frac{\tilde{R}}{\tilde{\omega}} (e_{\alpha\gamma\delta} p_{m_1\beta\gamma} + e_{\beta\gamma\delta} p_{m_1\alpha\gamma}) \\
& \times (\mathcal{H}_{m_2\delta} + \delta_{1m_2} \mathcal{H}_\delta^L) n_{m_3} n_{n-m_1-m_2-m_3}. \tag{23}
\end{aligned}$$

In Eqs. (21), (22), and (23) $\tilde{\omega} = \omega/\omega_p$ is the reduced laser frequency with respect to the bulk plasma frequency, $\tilde{R} = \omega_p R/c$ is the reduced cluster radius playing the role of the dipole-approximation parameter, and the dimensionless cluster parameter A is defined by Eq. (7). The vector term $V_{n\alpha}$ and the tensor term $T_{n\alpha\beta}$ on the right-hand sides of Eqs. (21a) and (21c), respectively, contain only nonlinear contributions of orders less than n . Therefore, they act as source terms for the n th-order quantities. We introduced the primes after the summation signs in Eqs. (22) and (23) in order to indicate that in these two sums the n th-order terms of all variables should be omitted. The dimensionless form of the Maxwell equations (20) inside the cluster is

$$\text{div } \mathcal{E}_n = -n_n, \quad \text{rot } \mathcal{E}_n = in\tilde{\omega}\tilde{R}\mathcal{H}_n, \tag{24a}$$

$$\text{div } \mathcal{H}_n = 0, \quad \text{rot } \mathcal{H}_n = -\tilde{\omega}\tilde{R}(in\mathcal{E}_n + \mathbf{q}_n). \tag{24b}$$

On the limiting integration sphere $\rho = \rho_{\text{lim}}$ the electric field of the n th-order harmonic, which is given by Eq. (17), may be presented in dimensionless form as

$$\mathcal{E}_n(t, \boldsymbol{\rho} = \rho_{\text{lim}} \mathbf{n}) = \frac{3\mathbf{n}(\mathbf{n} \cdot \mathbf{d}_n) - \mathbf{d}_n}{\epsilon_n(\rho_{\text{lim}})^3}, \tag{25}$$

where the dimensionless dipole moment \mathbf{d}_n corresponding to the n th-order harmonic is defined as

$$\mathbf{d}_n = \frac{\mathbf{d}^{(n0)}}{4\pi e z_i n_{\text{ion}} R^4} = - \int \boldsymbol{\rho} n_n \frac{d^3 \rho}{4\pi}. \tag{26}$$

Equations (21)–(24) constitute the complete set of equations, from which n th-order harmonic generation by the cluster can be determined, in principle. Note that they contain the dimensionless parameter \tilde{R} , whose smallness is the criterion of applicability of the dipole approximation. The condition $\tilde{R} \ll 1$ will be used in the solution of these equations. In particular, in the dipole approximation, which we consider, the terms with the magnetic field in Eqs. (22) and (23), which are proportional to \tilde{R} , can also be safely neglected. Besides, Maxwell's equations (24a) for the electric field can be approximated by $\text{rot } \mathcal{E}_n = 0$. Hence, the harmonic electric field \mathcal{E}_n can be derived from a potential φ_n , which satisfies the Poisson equation:

$$\mathcal{E}_n = -\nabla \varphi_n, \quad \Delta \varphi_n = n_n. \tag{27}$$

The hydrodynamic continuity equation (21a), together with the electrostatic equation (27), is equivalent to the equation

$$\mathbf{q}_n + in\mathcal{E}_n = -\text{rot } \mathbf{h}_n. \tag{28}$$

This is just the curl equation from Eqs. (24b), in which the magnetic vector function $\mathbf{h}_n \equiv \mathcal{H}_n/(\tilde{\omega}\tilde{R})$ satisfying the condition $\text{div } \mathbf{h}_n = 0$ should be self-consistently defined.

In solving Eqs. (21a) and (21c), we should discriminate between two cases. Because the cluster parameter A is generally very small, as was estimated in the previous Sec. II, the approximation $A = 0$ seems to be rather good, at least within some range of the laser electric-field strength to be defined below. In this case, if we assume $A = 0$, the term with the electron pressure tensor $p_{n\alpha\beta}$ is eliminated from Eq. (21b), and Eq. (21c) becomes redundant. Then, with the help of Eq. (21b) the electron current \mathbf{q}_n can be explicitly expressed as

$$\mathbf{q}_n = \frac{i\tilde{\omega}^2 \mathbf{V}_n}{n_0^2(n\tilde{\omega}^2 + i\gamma\tilde{\omega})} + \frac{n_0(\mathcal{E}_n + \delta_{1n}\mathcal{E}^L) + n_n\mathcal{E}_0}{i(n\tilde{\omega}^2 + i\gamma\tilde{\omega})}, \tag{29}$$

and using Eq. (28) we arrive at

$$\begin{aligned}
& \frac{i(n_0 - n^2\tilde{\omega}^2 - in\gamma\tilde{\omega})\mathcal{E}_n + in_0\delta_{1n}\mathcal{E}^L + in_n\mathcal{E}_0}{(n\tilde{\omega}^2 + i\gamma\tilde{\omega})} \\
& = \frac{i\tilde{\omega}^2 \mathbf{V}_n}{n_0^2(n\tilde{\omega}^2 + i\gamma\tilde{\omega})} + \text{rot } \mathbf{h}_n, \tag{30}
\end{aligned}$$

which should be solved together with Eq. (27) and the corresponding boundary conditions. At first glance, applicability of perturbation theory in the case of $A = 0$ is governed by the criterion $\mathcal{E}_L = E_L/(4\pi e z_i n_{\text{ion}} R) \ll 1$. Formally, this ensures that the linear approximation is small compared with the zeroth-order static case. For the nonlinear terms, however, the cluster radius R should be replaced by the surface diffuseness σ , so that the criterion is stronger and should read $E_L \ll 4\pi e z_i n_{\text{ion}} \sigma$. This was shown already for nanofilms in Ref. [60] and will hold here as well, at least for neutral nanoclusters. This is due to the increasing role of the density gradient in the nonlinear effects, which is maximal near the cluster surface. The modified condition can be written in the equivalent form $eE_L/(m_e\omega_p^2) \ll \sigma$, which is the condition for the classical threshold of plasma wave-breaking in the nonrelativistic regime [66]. This means that the electron oscillation amplitude inside the cluster should be smaller than the cluster surface thickness σ , which defines the minimal scale of the electron density inhomogeneity in the case of $A = 0$. Note that in the limit of a steplike cluster surface, viz. for $\sigma = 0$, the range of applicability of this perturbation theory formally disappears. Indeed, it means that in this case the quantum spill-out length of the electrons should replace σ in the above applicability criterion, but the quantum spill-out effect is outside this article.

Since the cluster parameter A is always quite small, one might expect that a nonzero value of A will only induce small corrections to the solution obtained in the approximation of $A = 0$. However, whether this statement is correct depends on the intensity of the incident laser field. If the latter is sufficiently small, the terms that are proportional to A may play a significant role. In Eqs. (21)–(24), as well as in the static Eqs. (6) we can perform a scaling transformation through the definitions $\tilde{\rho} = \rho/\sqrt{A}$, $\tilde{\mathcal{E}}_n = \mathcal{E}_n/\sqrt{A}$, $\tilde{q}_n = q_n/\sqrt{A}$, $\tilde{\mathcal{E}}^L = \mathcal{E}^L/\sqrt{A}$, and $\tilde{V}_n = V_n/\sqrt{A}$. Then, in terms of the tilded variables, Eqs. (6) and Eqs. (21)–(24) have the same form as before, but with the parameter A replaced by unity. In this case, the applicability of perturbation theory should be governed by the condition $\mathcal{E}_L = E_L/(4\pi e z_i n_{\text{ion}} R) \ll \sqrt{A}$, that is by the conditions $E_L \ll 4\pi e z_i n_{\text{ion}} l_Q$ or $E_L \ll 4\pi e z_i n_{\text{ion}} l_D$ for cold or laser-heated clusters, respectively. Again, these conditions can be rewritten as $eE_L/(m_e \omega_p^2) \ll l_Q$ or $eE_L/(m_e \omega_p^2) \ll l_D$, respectively, that is in the form of the classical wave-breaking threshold condition [66] for the case of $A \neq 0$, with l_Q or l_D playing the role of the minimal scale of the electron-density inhomogeneity, that is the minimal scale of the charge separation both near and inside the diffuse cluster surface in

the static limit. In the formal limit of $A \rightarrow 0$ the range of applicability of this perturbation expansion goes to zero. On the other hand, in the range of $(4\pi e z_i n_{\text{ion}} R)\sqrt{A} \ll E_L \ll 4\pi e z_i n_{\text{ion}} \sigma$ we retrieve the former expansion developed in the CCA.

For rather weak electromagnetic fields that satisfy the perturbation-theory condition in the case of $A \neq 0$, the n th-order contribution to the electron pressure tensor $p_{n\alpha\beta}$ can be expressed from the scale-transformed Eq. (21c) as

$$p_{n\alpha\beta} = \frac{i}{n} \left\{ \frac{T_{n\alpha\beta}}{n_0^2} - n_0^{a-1} \left(\frac{\partial \tilde{q}_{n\beta}}{\partial \tilde{\rho}_\alpha} + \frac{\partial \tilde{q}_{n\alpha}}{\partial \tilde{\rho}_\beta} + \frac{\partial \tilde{q}_{n\gamma}}{\partial \tilde{\rho}_\gamma} \delta_{\alpha\beta} \right) + n_0^{a-2} n'_0 \{ \tilde{q}_{n\beta} n_\alpha + \tilde{q}_{n\alpha} n_\beta + (1-a) \tilde{q}_{n\gamma} n_\gamma \delta_{\alpha\beta} \} \right\}, \quad (31)$$

where the equation of state for the electron gas was already taken into account in the form of the power law $p_0 = (n_0)^a$, with $a = 5/3$ for cold metal clusters and $a = 1$ for hot laser heated/ionized clusters. Then, after substituting this expression into the scale-transformed Eq. (21b) we arrive at an equation for the scaled electron-current components:

$$\begin{aligned} & n_0^{a-1} \left(2 \frac{\partial^2 \tilde{q}_{n\beta}}{\partial \tilde{\rho}_\alpha \partial \tilde{\rho}_\beta} + \frac{\partial^2 \tilde{q}_{n\alpha}}{\partial \tilde{\rho}_\beta^2} \right) - n_0^{a-2} n'_0 \left((2-a) \frac{\partial \tilde{q}_{n\alpha}}{\partial \tilde{\rho}_\beta} n_\beta + (2-a) \frac{\partial \tilde{q}_{n\beta}}{\partial \tilde{\rho}_\beta} n_\alpha - (2a-2) \frac{\partial \tilde{q}_{n\beta}}{\partial \tilde{\rho}_\alpha} n_\beta \right) \\ & - \tilde{q}_{n\alpha} n_0^{a-2} \left(n_0'' - \frac{(2-a)(n_0')^2}{n_0} + \frac{(4-a)n_0'}{\rho} \right) - (2-a) (\tilde{q}_{n\beta} n_\beta) n_\alpha n_0^{a-2} \left(n_0'' - \frac{(2-a)(n_0')^2}{n_0} - \frac{n_0'}{\rho} \right) \\ & + (n^2 \tilde{\omega}^2 + i n \gamma \tilde{\omega}) \tilde{q}_{n\alpha} + i n n_0 (\tilde{\mathcal{E}}_{n\alpha} + \delta_{1n} \tilde{\mathcal{E}}_\alpha^L) + i n n_n \tilde{\mathcal{E}}_{0\alpha} = \frac{i n \tilde{\omega}^2 \tilde{V}_{n\alpha}}{n_0^2} + \frac{\partial}{\partial \tilde{\rho}_\beta} \left(\frac{T_{n\alpha\beta}}{n_0^2} \right). \end{aligned} \quad (32)$$

This equation complemented by the analogs of Eqs. (27) and (28) in the scaled variables, that is by the equations

$$\tilde{\mathcal{E}}_n = -\nabla \tilde{\varphi}_n, \quad \Delta \tilde{\varphi}_n = n_n, \quad (33)$$

$$\tilde{q}_n + i n \tilde{\mathcal{E}}_n = -\text{rot } \tilde{h}_n, \quad \text{div } \tilde{h}_n = 0, \quad (34)$$

together forms the complete set of equations that should be solved with the corresponding boundary conditions to characterize the n th-order harmonic generation by the cluster.

IV. LINEAR RESPONSE OF THE FREE-ELECTRON NANOCLUSTER WITH DIFFUSE SURFACE

First, we consider the approximation $A = 0$ (the CCA), which is simpler and independent of the equation of state. Here the electron current is defined by the algebraic Eq. (29), rather than by a differential equation. But even in this case, Eqs. (27) and (30) are rather complicated for a general solution, in particular, due to the cumbersome right-hand term with $V_{n\alpha}$ in Eq. (30), not to speak of the case beyond the CCA. However, at least the problem of third-harmonic generation by the cluster, which is important for various applications, as well as the problem of nonlinear absorption in the first nonvanishing order of perturbation theory can be inspected. This will be

considered in a separate article. In this article, we consider in detail the linear case of $n = 1$, which is of interest in itself and will also serve as the basis for the nonlinear problems.

A. Linear response of the cluster in the CCA ($A = 0$)

In the linear case we have $V_1 \equiv 0$, even with allowance for the magnetic-field term in Eq. (22). The linear corrections to the electron potential, the electron density, and the magnetic \mathbf{h} function inside a spherical cluster can be represented as

$$\varphi_1 = (\mathcal{E}^L \cdot \mathbf{n}) u_1(\rho), \quad n_1 = (\mathcal{E}^L \cdot \mathbf{n}) v_1(\rho), \quad (35a)$$

$$\mathbf{h}_1 = [\mathcal{E}^L \times \mathbf{n}] w_1(\rho). \quad (35b)$$

Then

$$\mathcal{E}_1 = -\nabla \varphi_1 = -(u_1/\rho) \mathcal{E}_\perp^L - u_1' \mathbf{n} (\mathcal{E}^L \cdot \mathbf{n}), \quad (36a)$$

$$\text{rot } \mathbf{h}_1 = (w_1' + w_1/\rho) \mathcal{E}_\perp^L + (2w_1/\rho) \mathbf{n} (\mathcal{E}^L \cdot \mathbf{n}), \quad (36b)$$

$$\mathbf{q}_1 = q_{1\perp}(\rho) \mathcal{E}_\perp^L + q_{1\parallel}(\rho) \mathbf{n} (\mathcal{E}^L \cdot \mathbf{n}), \quad (36c)$$

with $\mathcal{E}_\perp^L = \mathcal{E}^L - \mathbf{n} (\mathcal{E}^L \cdot \mathbf{n})$ and, from Eq. (29),

$$q_{1\perp} = \frac{n_0(1 - u_1/\rho)}{i(\tilde{\omega}^2 + i\gamma\tilde{\omega})}, \quad q_{1\parallel} = \frac{n_0(1 - u_1') + \mathcal{E}_0 v_1}{i(\tilde{\omega}^2 + i\gamma\tilde{\omega})}. \quad (37)$$

Finally, from Eqs. (27) and (30) we obtain three differential equations for the scalar spherically symmetric functions $u_1(\rho)$, $v_1(\rho)$, and $w_1(\rho)$:

$$\frac{i(n_0 - \tilde{\omega}^2 - i\gamma\tilde{\omega})(-u_1/\rho) + in_0}{(\tilde{\omega}^2 + i\gamma\tilde{\omega})} = w_1' + \frac{w_1}{\rho}, \quad (38a)$$

$$\frac{i(n_0 - \tilde{\omega}^2 - i\gamma\tilde{\omega})(-u_1') + in_0 + iv_1\mathcal{E}_0}{(\tilde{\omega}^2 + i\gamma\tilde{\omega})} = \frac{2w_1}{\rho}, \quad (38b)$$

$$u_1'' + 2u_1'/\rho - 2u_1/\rho^2 = v_1. \quad (38c)$$

With Eqs. (35) and (38c), the first-order dipole moment \mathbf{d}_1 from Eq. (26) can be presented as

$$\mathbf{d}_1 = -\frac{1}{3}\mathcal{E}^L \int_0^{\rho_{\text{lim}}} v_1(\rho)\rho^3 d\rho = -\frac{1}{3}\mathcal{E}^L(\rho_{\text{lim}})^3 \times \{u_1'(\rho_{\text{lim}}) - u_1(\rho_{\text{lim}})/\rho_{\text{lim}}\} \equiv \alpha_1 \mathcal{E}^L, \quad (39)$$

where always $\rho_{\text{lim}} = 1 + \sigma/(2R)$ for the current case of the CCA and $\alpha_1 = -(\rho_{\text{lim}})^3 \{u_1'(\rho_{\text{lim}}) - u_1(\rho_{\text{lim}})/\rho_{\text{lim}}\}/3$ is the dimensionless linear polarizability of the cluster. In terms of this, the linear cross sections σ_{1sc} and σ_{1ab} for scattering and absorption, respectively, of the incident laser wave with intensity I_0 can be represented in dimensionless form:

$$\sigma_{\text{1sc}}/(\pi R^2) = \frac{8}{3} \left(\frac{2 + \epsilon_1}{3} \right)^2 \left(\frac{\omega_p R}{c} \right)^4 \tilde{\omega}^4 |\alpha_1|^2, \quad (40a)$$

$$\sigma_{\text{1ab}}/(\pi R^2) = \frac{4\omega_p R}{c\sqrt{\epsilon_1}} \left(\frac{2 + \epsilon_1}{3} \right)^2 \tilde{\omega} \text{Im}\alpha_1. \quad (40b)$$

Knowing the reduced cross sections of linear scattering and absorption, $\tilde{\omega}^4 |\alpha_1|^2$ and $\tilde{\omega} \text{Im}\alpha_1$, respectively, permits one easily to obtain the dimensional cross sections for any cluster parameters R and ω_p .

The system of Eqs. (38) requires three boundary conditions for its solution. Equating the tangential components of the electric field on either side of the exterior cluster boundary, from Eqs. (25) and (36a) the boundary condition for the function $u_1(\rho)$ at $\rho = \rho_{\text{lim}}$ can be obtained:

$$u_1'(\rho_{\text{lim}}) = (1 - 3\epsilon_1)u_1(\rho_{\text{lim}})/\rho_{\text{lim}}, \quad (41)$$

which also can be regarded as a consequence of the continuity of the electric potential. The other two boundary conditions to Eqs. (38) are $u_1(0) = 0$ and $w_1(0) = 0$, with $u_1 \sim \rho$ and $w_1 \sim \rho$ as $\rho \rightarrow 0$. Recall that, for the case of a neutral cluster in the approximation of $A = 0$, we have $\mathcal{E}_0(\rho) = 0$ throughout the whole cluster and only the two first-order differential equations (38a) and (38b) need be solved. In this case, they can be reduced to the single second-order equation

$$u_1'' + \frac{n_0' u_1'}{n_0 - \tilde{\omega}^2 - i\gamma\tilde{\omega}} + \frac{2u_1'}{\rho} - \frac{2u_1}{\rho^2} = \frac{n_0'}{n_0 - \tilde{\omega}^2 - i\gamma\tilde{\omega}}. \quad (42)$$

Generally, Eqs. (38) or Eq. (42) require a numerical solution. However, in the cluster bulk for a neutral cluster for $\rho < 1 - \sigma/(2R)$, where $n_0 = 1$ and $\mathcal{E}_0 = 0$, the exact solution of Eqs. (38) is the linear dependence $u_1 = C_u \rho$, $w_1 = C_w \rho$, with $C_w = i[1 - C_u(1 - \tilde{\omega}^2 - i\gamma\tilde{\omega})]/[2(\tilde{\omega}^2 + i\gamma\tilde{\omega})]$. In consequence, in this range $v_1 = 0$ and $n_1 = 0$, and this bulk range of the cluster does not contribute to the cluster dipole moment.

Only the surface range $1 - \sigma/(2R) < \rho < 1 + \sigma/(2R)$ contributes to the dipole moment. Here the ion/electron density is inhomogeneous and the solution of Eqs. (38) or Eq. (42) should be obtained numerically. Note that the result for the steplike cluster boundary of a neutral cluster can be obtained in this model only as the limiting case of $\sigma/R \rightarrow +0$, but not for $\sigma \equiv 0$. For a neutral cluster, this confirms the importance of the cluster surface for the description of the linear Mie resonance as essentially a surface-plasmon excitation.

For charged clusters, we may discriminate two cases. If the radius R_c of the neutral core defined by Eq. (10) satisfies the condition $R_c/R \equiv \rho_c > 1 - \sigma/(2R)$, that is, in the case of a low outer-ionization degree, the situation is qualitatively similar to the case of a neutral cluster, with some quantitative difference due to the presence of the outer positively charged zone of the diffuse cluster surface. On the other hand, in the case of a high outer-ionization degree it may be that $R_c/R \equiv \rho_c < 1 - \sigma/(2R)$, that is, the diffuse cluster surface together with a part of the bulk is completely depleted of electrons. In this case, the analytical solution of Eqs. (38) can be obtained. As was the case for neutral clusters above, for highly charged clusters in the range where $\rho \leq \rho_c$ the exact solution of Eqs. (38) is the linear dependence $u_1 = C_u \rho$, $w_1 = C_w \rho$, with $C_w = i[1 - C_u(1 - \tilde{\omega}^2 - i\gamma\tilde{\omega})]/[2(\tilde{\omega}^2 + i\gamma\tilde{\omega})]$. On the other hand, in the range $\rho_c < \rho < 1 + \sigma/(2R)$, where $n_0 = 0$, the solution is $u_1 = B_u/\rho^2 + D_u \rho$ and $w_1 = B_w/\rho^2 + D_w \rho$, with $B_w = -iB_u$ and $D_w = iD_u/2$. Here, the function v_1 , as well as the first-order electron density n_1 are zero everywhere, except at the point $\rho = \rho_c$, where they have a Dirac δ function singularity due to discontinuity of u_1' . The three unknown coefficients C_u , B_u , and D_u can be found from the two continuity conditions on the functions u_1 and w_1 at $\rho = \rho_c$, and from the boundary condition (41) at $\rho = \rho_{\text{lim}} = 1 + \sigma/(2R)$. In this, the linear cluster polarizability is $\alpha_1 = B_u$, and the final result reads

$$\alpha_1 = \frac{\epsilon_1 \rho_c^3}{\epsilon_1 + (1 - \epsilon_1)(\rho_c/\rho_{\text{lim}})^3 - 3\epsilon_1(\tilde{\omega}^2 + i\gamma\tilde{\omega})}. \quad (43)$$

For the sake of generality, an arbitrary permittivity ϵ_1 is kept in Eq. (43), which originates from the boundary condition (41). This allows us also to consider from Eq. (43) the case of a neutral cluster with steplike boundary surrounded by a dielectric, as a limiting case of a highly charged cluster at $\eta \rightarrow 0$ and $\sigma/R \rightarrow 0$. But first, if we let $\epsilon_1 = 1$ in Eq. (43), we arrive at the cluster polarizability $\alpha_1 = \rho_c^3/[1 - 3(\tilde{\omega}^2 + i\gamma\tilde{\omega})]$ for a charged cluster in vacuum with diffuse boundary at high outer-ionization degree. This result means that the outer-ionization degree of a highly charged cluster does not affect the Mie-resonance frequency, which for a cluster in vacuum continues to have the classical value $\omega_M^{(cl)} = \omega_p/\sqrt{3}$ (in the limit of $\gamma \rightarrow 0$). It is only the strength of the Mie-plasmon resonance that decreases with increasing outer-ionization degree, that is, with decreasing dimensionless neutral-core radius $\rho_c = R_c/R$ of the charged cluster. On the other hand, if we assume $\sigma/R = 0$ and then let $\rho_c = \rho_{\text{lim}} = 1$ in Eq. (43) with an arbitrary ϵ_1 , we arrive at the cluster polarizability $\alpha_1 = \epsilon_1/[1 - 3\epsilon_1(\tilde{\omega}^2 + i\gamma\tilde{\omega})]$ for a neutral cluster with steplike surface in a dielectric medium. In this case, the Mie-resonance frequency following from this expression for cluster polarizability is $\omega_M = \omega_p/\sqrt{3\epsilon_1}$ (for $\gamma \rightarrow 0$), which does not exactly coincide

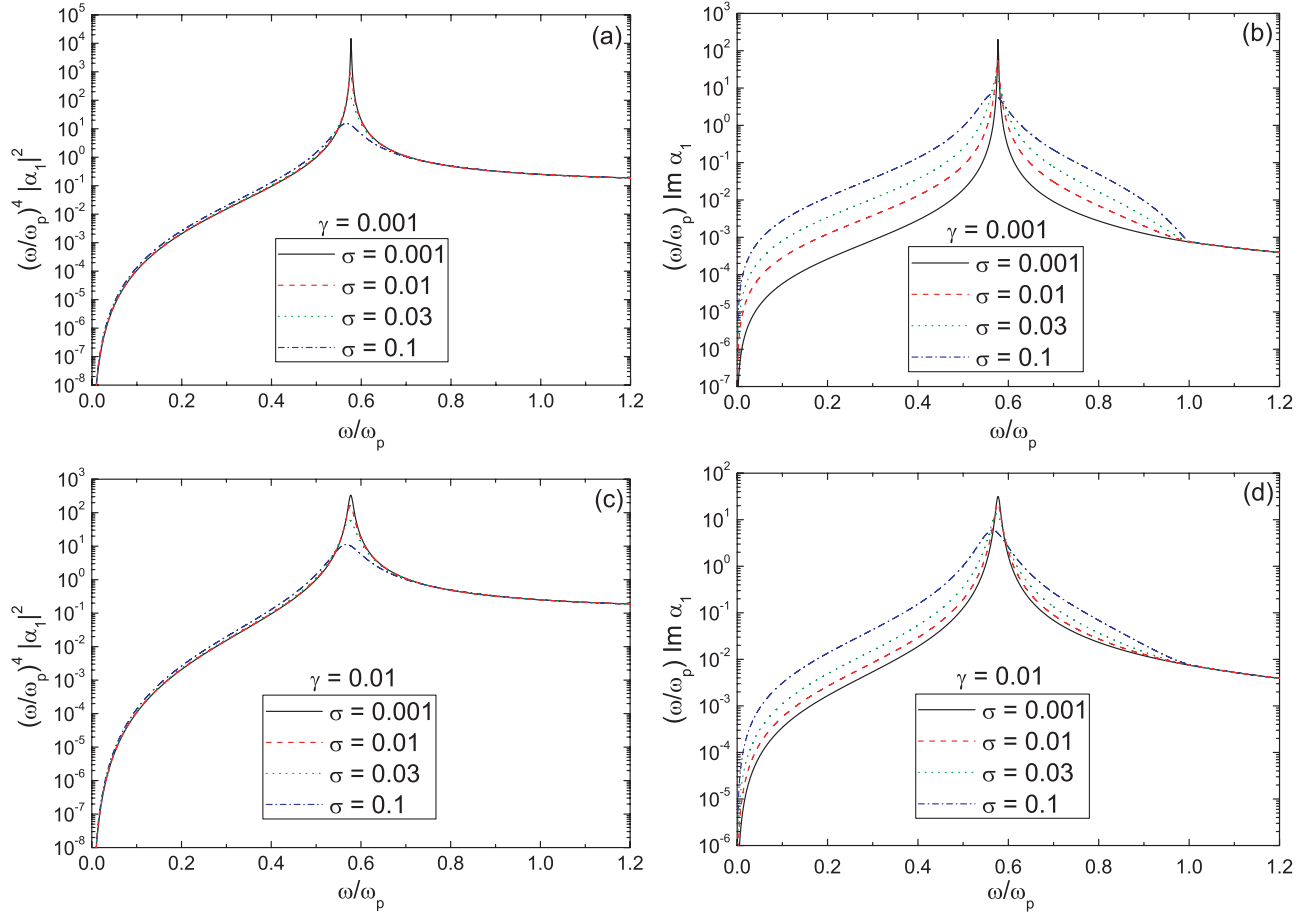


FIG. 3. (Color online) The reduced cross sections of linear scattering and absorption, respectively, $\tilde{\omega}^4 |\alpha_1|^2$ [(a) and (c)] and $\tilde{\omega} \text{Im} \alpha_1$ [(b) and (d)], as a result of numerical solution of Eqs. (38) for a neutral cluster ($\eta = 0$) within the CCA ($A = 0$), for $\epsilon_1 = 1$, for $\gamma = 10^{-3}$ [(a) and (b)] and $\gamma = 10^{-2}$ [(c) and (d)], and for different cluster surface thicknesses. In each panel, the four curves correspond to $\sigma/R = 10^{-3}$ (the solid curves), $\sigma/R = 10^{-2}$ (the dashed curves), $\sigma/R = 3 \times 10^{-2}$ (the dotted curves), and $\sigma/R = 10^{-1}$ (the dash-dotted curves). For the ion density of the cluster surface region, the completely smooth profile $g_5(x)$ is used (see Fig. 1).

with the classical textbook expression $\omega_M^{(cl)} = \omega_p / \sqrt{1 + 2\epsilon_1}$ for the Mie-resonance frequency of a neutral metal cluster in a dielectric [10,67].

To understand the difference between our result for the plasmon Mie-resonance frequency of a free-electron nanocluster in a dielectric and the textbook result, let us recall that the latter has been obtained by simply extrapolating the electrostatic cluster polarizability $\alpha_{1st} = (\epsilon_{cl-st} - \epsilon_{1st}) / (\epsilon_{cl-st} + 2\epsilon_{1st})$ to the dynamic case, by means of the substitutions $\epsilon_{cl-st} \rightarrow \epsilon_{cl}(\omega) = 1 - 1/[\tilde{\omega}^2 + i\gamma\tilde{\omega}]$ and $\epsilon_{1st} \rightarrow \epsilon_1(\omega)$. Then, in this electrostatic approximation the cluster polarizability becomes $\alpha_1 = [1 - (1 - \epsilon_1)(\tilde{\omega}^2 + i\gamma\tilde{\omega})] / [1 - (1 + 2\epsilon_1)(\tilde{\omega}^2 + i\gamma\tilde{\omega})]$, from which the above-mentioned classical result for the Mie-resonance frequency is directly obtained. On the other hand, here we exploit the fully dynamical approach, in which the role of the magnetic field is significant. Even though it is small in the dipole approximation, the magnetic field enters the dynamic Eqs. (38) through the magnetic \mathbf{h} function, on the same footing with the electric potential. Apparently, this is the main difference between our approach and the pure electrostatic approximation, thus this is what led to different expressions for the plasmon Mie-resonance frequency of a free-electron nanocluster embedded

in a surrounding dielectric medium. While this difference is important in principle, the quantitative difference between the two Mie-resonance frequencies is not too large for realistic moderate values of the permittivity ϵ_1 of the surrounding dielectric.

To illustrate the above statements, the numerical solution of Eqs. (38) for various cases was used to calculate $\tilde{\omega} \text{Im} \alpha_1$ and $\tilde{\omega}^4 |\alpha_1|^2$ and thereby the reduced cross sections for linear absorption and scattering, respectively [cf. Eqs. (40)]. The results are presented in Figs. 3–6. In Fig. 3, the results for a neutral cluster ($\eta = 0$) in vacuum ($\epsilon_1 = 1$) for different cluster-surface thicknesses are exhibited. In Figs. 3(a) and 3(b) the results of calculations with a value of the relaxation constant $\gamma = 10^{-3}$ [cf. Eq. (1b) and the discussion below Eq. (2)] are presented. Clearly, the absorption as well as the scattering cross section reveal resonance behavior with a maximum at $\tilde{\omega} \approx 0.577$ for sufficiently small values of the relative cluster-surface thickness $\sigma/R \lesssim 0.001$, demonstrating precise agreement with the classical Mie-resonance frequency in vacuum $\omega_M^{(cl)} = \omega_p / \sqrt{3}$. With σ/R increasing up to 0.1, a small but visible red shift of the resonance frequency can be noticed. Also, with increasing σ/R , some broadening of the resonance curve both for absorption and for scattering takes

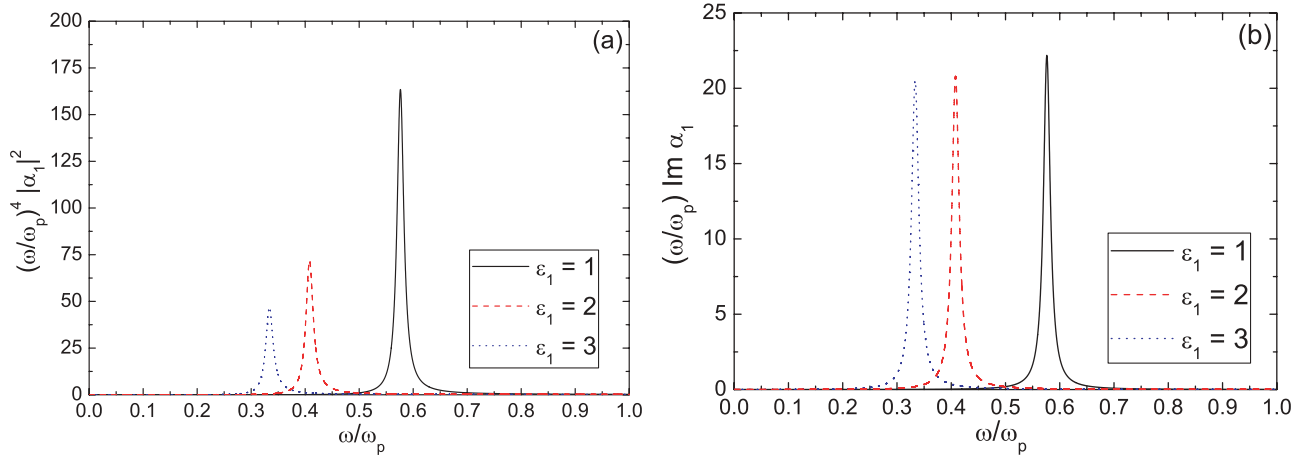


FIG. 4. (Color online) The reduced cross sections of linear scattering and absorption, respectively, (a) $\tilde{\omega}^4 |\alpha_1|^2$ and (b) $\tilde{\omega} \text{Im} \alpha_1$, as a result of numerical solution of Eqs. (38) for a neutral cluster ($\eta = 0$) within the CCA ($A = 0$) for $\sigma/R = 0.01$ and with $\gamma = 10^{-2}$, and for different dielectric permittivities ϵ_1 of the surrounding. In each panel, the three curves correspond to $\epsilon_1 = 1$ (the solid curves), $\epsilon_1 = 2$ (the dashed curves), and $\epsilon_1 = 3$ (the dotted curves). For the ion density of the cluster surface region, the completely smooth profile $g_5(x)$ is used (see Fig. 1).

place. For absorption, this implies a very significant increase in both wings of the resonance profile, to the left and to the right of the Mie-resonance frequency but not exceeding the bulk plasma resonance frequency at $\tilde{\omega} = 1$. This enhancement of the absorption with increasing σ/R has the same physical origin as in the case of thin nanofilms with diffuse boundaries, which was considered in detail in Ref. [60]. Basically, it is connected with resonant volume absorption inside the diffuse cluster surface: in our model, the *local* plasma frequency rises continuously from a value of zero up to the bulk plasma frequency. Therefore, within this frequency range, there is always resonant absorption in some part of the diffuse surface region. Qualitatively the same results are obtained for the higher value of the relaxation constant, $\gamma = 0.01$. They are presented in Figs. 3(c) and 3(d) for comparison.

Figure 4 displays results obtained for a neutral cluster embedded into a dielectric surrounding. They show that the resonance frequency both for scattering and for absorption shifts toward lower frequencies with increasing dielectric permittivity ϵ_1 of the surrounding, in rather good qualitative agreement with the classical Mie-resonance frequency in a dielectric $\omega_M^{(cl)} = \omega_p / \sqrt{1 + 2\epsilon_1}$ [10,67], which is obtained in the electrostatic approximation. Quantitatively, however, the resonance frequency obtained in our calculations reveals a noticeable red shift with respect to the classical Mie frequency if $\epsilon_1 \neq 1$ and, indeed, it is in excellent quantitative agreement with the plasmon Mie-resonance frequency $\omega_M = \omega_p / \sqrt{3\epsilon_1}$ derived above. The relative red shift with respect to the classical Mie frequency as a function of ϵ_1 extracted from the calculations of the resonance curves is presented in Fig. 5 for the case of relative surface diffuseness $\sigma/R = 0.01$ and $\gamma = 10^{-2}$, as in Fig. 4. In this case, there is no red shift for a cluster in vacuum, at $\epsilon_1 = 1$. It gradually increases with increasing ϵ_1 , and is of the order of 10% for $2 < \epsilon_1 < 3$ as compared with the classical Mie frequency.

Figure 6 exhibits the results obtained for a charged cluster in vacuum ($\epsilon_1 = 1$), for $\gamma = 10^{-2}$ and $\sigma/R = 0.03$. The critical value η_c of the outer-ionization degree $\eta \equiv \eta(R_c/R)$, which

separates the ranges of low and high ionization degrees in the CCA, is defined so that the radius of the neutral core R_c coincides with the radius of the inner boundary of the diffuse cluster surface, which corresponds to the condition

$$R_c/R = 1 - \sigma/(2R), \quad (44)$$

and thus $\eta_c \equiv \eta|_{r=1-\sigma/(2R)}$, where $r = R_c/R$. In this case, we find $\eta_c \approx 0.0445$. Figure 6 shows a noticeable difference of the resonance curves, especially for absorption, for a neutral cluster as compared with a charged cluster for high outer-ionization degrees $\eta > \eta_c$. The difference appears chiefly in a drastic narrowing of the resonance curves at $\eta > \eta_c$, because in this case the diffuse cluster surface no longer plays the decisive role in forming the electromagnetic cluster response. A further increase of the outer-ionization degree results in a gradual decrease of both scattering and absorption because the number

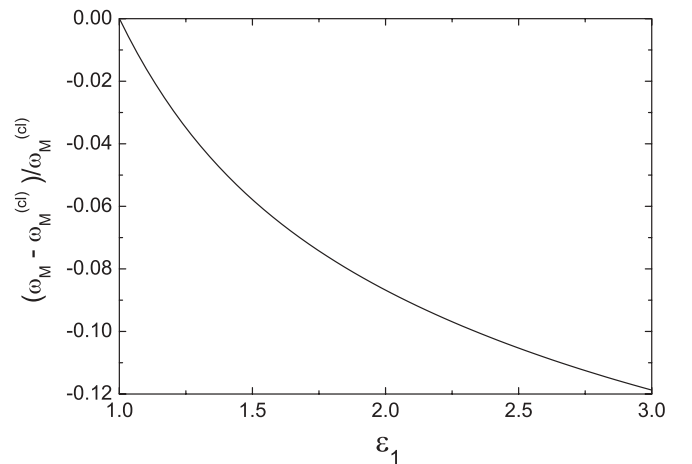


FIG. 5. The relative shift of the calculated resonance Mie frequency ω_M of the metal cluster embedded into a dielectric surrounding with permittivity ϵ_1 with respect to the classical Mie frequency $\omega_M^{(cl)} = \omega_p / \sqrt{1 + 2\epsilon_1}$ as a function of ϵ_1 . As in Fig. 4, $\sigma/R = 0.01$ and $\gamma = 10^{-2}$.

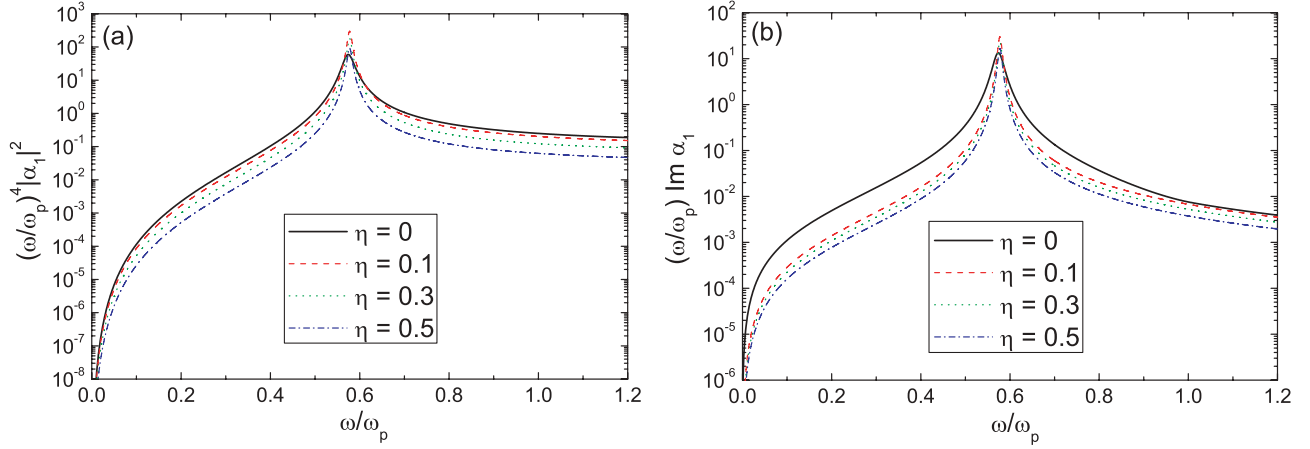


FIG. 6. (Color online) The reduced cross sections of linear scattering and absorption, respectively, (a) $\tilde{\omega}^4 |\alpha_1|^2$ and (b) $\tilde{\omega} \text{Im} \alpha_1$, as a result of the numerical solution of Eqs. (38) for a charged cluster in vacuum ($\epsilon_1 = 1$) within the CCA ($A = 0$) for $\sigma/R = 0.03$ and with $\gamma = 10^{-2}$ and for various outer ionization degrees η . In each panel, the four curves correspond to the following values of η : $\eta = 0$ (solid curves), $\eta = 0.1$ (dash curves), $\eta = 0.3$ (dot curves), and $\eta = 0.5$ (dash-dot curves). For the ion density of the cluster surface region, the completely smooth profile $g_5(x)$ is used (see Fig. 1).

of trapped electrons in the charged cluster is decreasing. On the other hand, the position of the Mie resonance for charged clusters is hardly changed from its value for neutral clusters. For highly charged clusters within the CCA (at $A = 0$), we actually deal with the steplike case with respect to the neutral core of the cluster. But this should no longer hold when $A \neq 0$, due to the diffuseness of the transition range between the neutral core and the charged shell in a highly ionized cluster.

B. Linear response of the cluster beyond the CCA ($A \neq 0$)

In this case we have again $\tilde{\mathbf{V}}_1 \equiv 0$, and also $T_{1\alpha\beta} = 0$, even with allowance for the magnetic field terms in Eqs. (22) and (23). The linear corrections to the scale-transformed electron potential, the electron density, and the magnetic $\tilde{\mathbf{h}}$ function inside the spherical cluster can be represented through three scalar functions as before in the case of $A = 0$:

$$\tilde{\varphi}_1 = (\tilde{\mathcal{E}}^L \cdot \mathbf{n}) \tilde{u}_1(\tilde{\rho}), \quad n_1 = (\tilde{\mathcal{E}}^L \cdot \mathbf{n}) \tilde{v}_1(\tilde{\rho}), \quad (45a)$$

$$\tilde{\mathbf{h}}_1 = [\tilde{\mathcal{E}}^L \times \mathbf{n}] \tilde{w}_1(\tilde{\rho}). \quad (45b)$$

Again, as in Eqs. (36), we have

$$\tilde{\mathcal{E}}_1 = -\nabla \tilde{\varphi}_1 = -(\tilde{u}_1/\tilde{\rho}) \tilde{\mathcal{E}}_1^L - \tilde{u}'_1 \mathbf{n} (\tilde{\mathcal{E}}^L \cdot \mathbf{n}), \quad (46a)$$

$$\text{rot } \tilde{\mathbf{h}}_1 = (\tilde{w}'_1 + \tilde{w}_1/\tilde{\rho}) \tilde{\mathcal{E}}_1^L + (2\tilde{w}_1/\tilde{\rho}) \mathbf{n} (\tilde{\mathcal{E}}^L \cdot \mathbf{n}), \quad (46b)$$

$$\tilde{\mathbf{q}}_1 = \tilde{q}_{1\perp}(\tilde{\rho}) \tilde{\mathcal{E}}_1^L + \tilde{q}_{1\parallel}(\tilde{\rho}) \mathbf{n} (\tilde{\mathcal{E}}^L \cdot \mathbf{n}), \quad (46c)$$

with $\tilde{\mathcal{E}}_1^L = \tilde{\mathcal{E}}^L - \mathbf{n} (\tilde{\mathcal{E}}^L \cdot \mathbf{n})$. From Eqs. (33) and (34) we obtain

$$i\tilde{u}'_1 = 2\tilde{w}_1/\tilde{\rho} + \tilde{q}_{1\parallel}, \quad (47a)$$

$$\tilde{w}'_1 = i\tilde{u}_1/\tilde{\rho} - \tilde{w}_1/\tilde{\rho} - \tilde{q}_{1\perp}, \quad (47b)$$

$$\tilde{u}''_1 + 2\tilde{u}'_1/\tilde{\rho} - 2\tilde{u}_1/\tilde{\rho}^2 = \tilde{v}_1, \quad (47c)$$

where, however, the electron current components $\tilde{q}_{1\perp}$ and $\tilde{q}_{1\parallel}$ obey the second-order differential equations following

from Eq. (32):

$$\begin{aligned} n_0^{a-1} \left\{ \tilde{q}''_{1\perp} + \frac{2(\tilde{q}'_{1\parallel} + \tilde{q}'_{1\perp})}{\tilde{\rho}} + \frac{6(\tilde{q}_{1\parallel} - \tilde{q}_{1\perp})}{\tilde{\rho}^2} \right\} - n_0^{a-2} n'_0 \\ \times \left\{ (2-a)\tilde{q}'_{1\perp} + \tilde{q}_{1\perp} \left[\frac{n''_0}{n'_0} - (2-a)\frac{n'_0}{n_0} \right] \right. \\ \left. + (2+a)\frac{\tilde{q}_{1\perp}}{\tilde{\rho}} + (2-2a)\frac{\tilde{q}_{1\parallel}}{\tilde{\rho}} \right\} \\ + (\tilde{\omega}^2 + i\gamma\tilde{\omega})\tilde{q}_{1\perp} + in_0(1 - \tilde{u}_1/\tilde{\rho}) = 0, \end{aligned} \quad (48a)$$

$$\begin{aligned} n_0^{a-1} \left\{ 3\tilde{q}''_{1\parallel} + \frac{6\tilde{q}'_{1\parallel} - 4\tilde{q}'_{1\perp}}{\tilde{\rho}} - \frac{8(\tilde{q}_{1\parallel} - \tilde{q}_{1\perp})}{\tilde{\rho}^2} \right\} - n_0^{a-2} n'_0 \\ \times \left\{ (6-4a)\tilde{q}'_{1\parallel} + (3-a)\tilde{q}_{1\parallel} \left[\frac{n''_0}{n'_0} - (2-a)\frac{n'_0}{n_0} \right] \right. \\ \left. + (6-2a)\frac{\tilde{q}_{1\parallel}}{\tilde{\rho}} - (4-2a)\frac{\tilde{q}_{1\perp}}{\tilde{\rho}} \right\} + (\tilde{\omega}^2 + i\gamma\tilde{\omega})\tilde{q}_{1\parallel} \\ + in_0(1 - \tilde{u}'_1) + i\tilde{v}_1\tilde{\mathcal{E}}_0 = 0. \end{aligned} \quad (48b)$$

From the scale-transformed static Eqs. (6), we have $n_0^{a-2} n'_0 = -\tilde{\mathcal{E}}_0/a$ and $n''_0/n'_0 - (2-a)n'_0/n_0 = \tilde{\mathcal{E}}'_0/\tilde{\mathcal{E}}_0$, with $\tilde{\mathcal{E}}'_0 = \Theta_i - n_0 - 2\tilde{\mathcal{E}}_0/\tilde{\rho}$.

Now, the first-order dipole moment \mathbf{d}_1 can be presented as

$$\begin{aligned} \mathbf{d}_1 = -\frac{A^2}{3} \tilde{\mathcal{E}}^L \int_0^{\tilde{\rho}_{\text{lim}}} \tilde{v}_1(\tilde{\rho}) \tilde{\rho}^3 d\tilde{\rho} = -\frac{A^{3/2}}{3} \mathcal{E}^L (\tilde{\rho}_{\text{lim}})^3 \\ \times \{ \tilde{u}'_1(\tilde{\rho}_{\text{lim}}) - \tilde{u}_1(\tilde{\rho}_{\text{lim}})/\tilde{\rho}_{\text{lim}} \} \equiv \alpha_1 \mathcal{E}^L, \end{aligned} \quad (49)$$

where $\tilde{\rho}_{\text{lim}} = \rho_{\text{lim}}/\sqrt{A}$. The dimensionless linear polarizability $\alpha_1 = -A^{3/2}(\tilde{\rho}_{\text{lim}})^3 \{ \tilde{u}'_1(\tilde{\rho}_{\text{lim}}) - \tilde{u}_1(\tilde{\rho}_{\text{lim}})/\tilde{\rho}_{\text{lim}} \}/3$ of the cluster is defined as in Eq. (39). This is consistent with the previous notation in the case of the CCA, so that Eqs. (40) for the linear cross sections for scattering and absorption again hold.

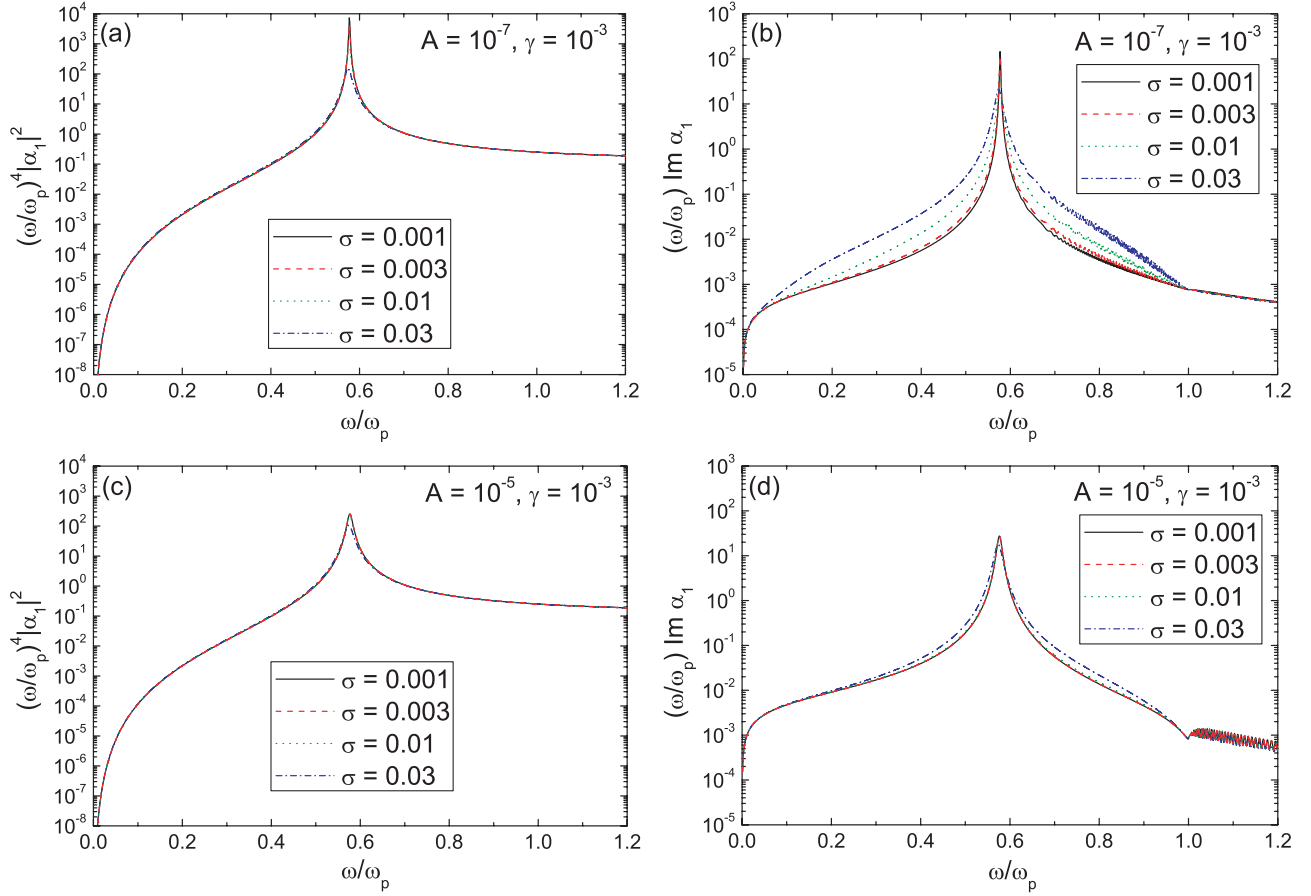


FIG. 7. (Color online) The reduced cross sections of linear scattering and absorption, respectively, $\tilde{\omega}^4 |\alpha_1|^2$ [(a) and (c)] and $\tilde{\omega} \text{Im} \alpha_1$ [(b) and (d)], as a result of the numerical solution of Eqs. (47) and (48) for cold neutral metal clusters with an electron halo in vacuum ($\epsilon_1 = 1$) beyond the CCA [$A = 10^{-7}$ for (a) and (b) and $A = 10^{-5}$ for (c) and (d)], with $\gamma = 10^{-3}$ and for various cluster-surface diffusenesses σ/R . In each panel the four calculated curves correspond to the following values of σ/R : $\sigma/R = 0.001$ (solid curves), $\sigma/R = 0.003$ (dash curves), $\sigma/R = 0.01$ (dot curves), and $\sigma/R = 0.03$ (dash-dot curves). For the ion density of the cluster surface region, the completely smooth profile $g_5(x)$ is used (see Fig. 1).

Equations (47a) and (47b) can be reduced to a single second-order equation

$$\tilde{u}_1'' + 2\tilde{u}_1'/\tilde{\rho} - 2\tilde{u}_1/\tilde{\rho}^2 = -i\tilde{q}'_{1\parallel} - \frac{2i(\tilde{q}'_{1\parallel} - \tilde{q}'_{1\perp})}{\tilde{\rho}}, \quad (50)$$

so the comparison with Eq. (47c) results in $\tilde{v}_1 = -i\tilde{q}'_{1\parallel} - 2i(\tilde{q}'_{1\parallel} - \tilde{q}'_{1\perp})/\tilde{\rho}$. Equation (50) requires two boundary conditions. They are the same as before in the CCA, namely $\tilde{u}_1(0) = 0$ and

$$\tilde{u}'_1(\tilde{\rho}_{\text{lim}}) = (1 - 3\epsilon_1)\tilde{u}_1(\tilde{\rho}_{\text{lim}})/\tilde{\rho}_{\text{lim}} \quad (51)$$

[here, the condition $\tilde{v}_1(0) = 0$ automatically holds in view of Eq. (47a)]. The four boundary conditions for the solution of Eqs. (48) are $\tilde{q}_{1\parallel}(\tilde{\rho}_{\text{lim}}) = 0$, $\tilde{q}_{1\parallel}(0) = \tilde{q}_{1\perp}(0)$, and $\tilde{q}'_{1\parallel}(0) = \tilde{q}'_{1\perp}(0) = 0$ (the latter also follows from the finiteness of both electron current components at the cluster center).

Equations (47) and (48) require a numerical solution. Equations (48) involve the static electron-density distribution n_0 and the static electric field \mathcal{E}_0 , which result from the solution of the static Eqs. (6), as well as their derivatives. Unlike in the previous case of the CCA, in the current case beyond the CCA cold metal clusters and hot laser-heated

clusters should be considered separately, as was the case for the static Eqs. (6). In this case both the equations and their solutions are equation-of-state dependent. This means they are primarily dependent on the parameter a defined by the power law $p_0 = (n_0)^a$ in the equilibrium equation of state for the electron gas. Besides, the results may differ, depending on whether an electron halo around the cluster in vacuum is assumed. For various situations, the results for the reduced cross sections for linear scattering and absorption obtained from the numerical solution of Eqs. (47) and (48) are presented below in Figs. 7–11.

In Figs. 7 and 8, the results for a neutral metal cluster ($\eta = 0$) in vacuum ($\epsilon_1 = 1$) for several values of the cluster-surface thickness and the cluster parameter A are presented and compared for two values of the relaxation constant, $\gamma = 10^{-3}$ (Fig. 7) and 10^{-2} (Fig. 8). For the calculations underlying these figures, spreading of the electron density beyond the cluster surface (the electron halo with an extent of the order of σ) was assumed to be possible both for the static and the dynamic solutions. Hence, in all these calculations we set ρ_{lim} to a large value, $\rho_{\text{lim}} \cong 8$, which assured that the electron density as well as the electron current are free to vanish on the limiting integration sphere without being forced by a constraint.

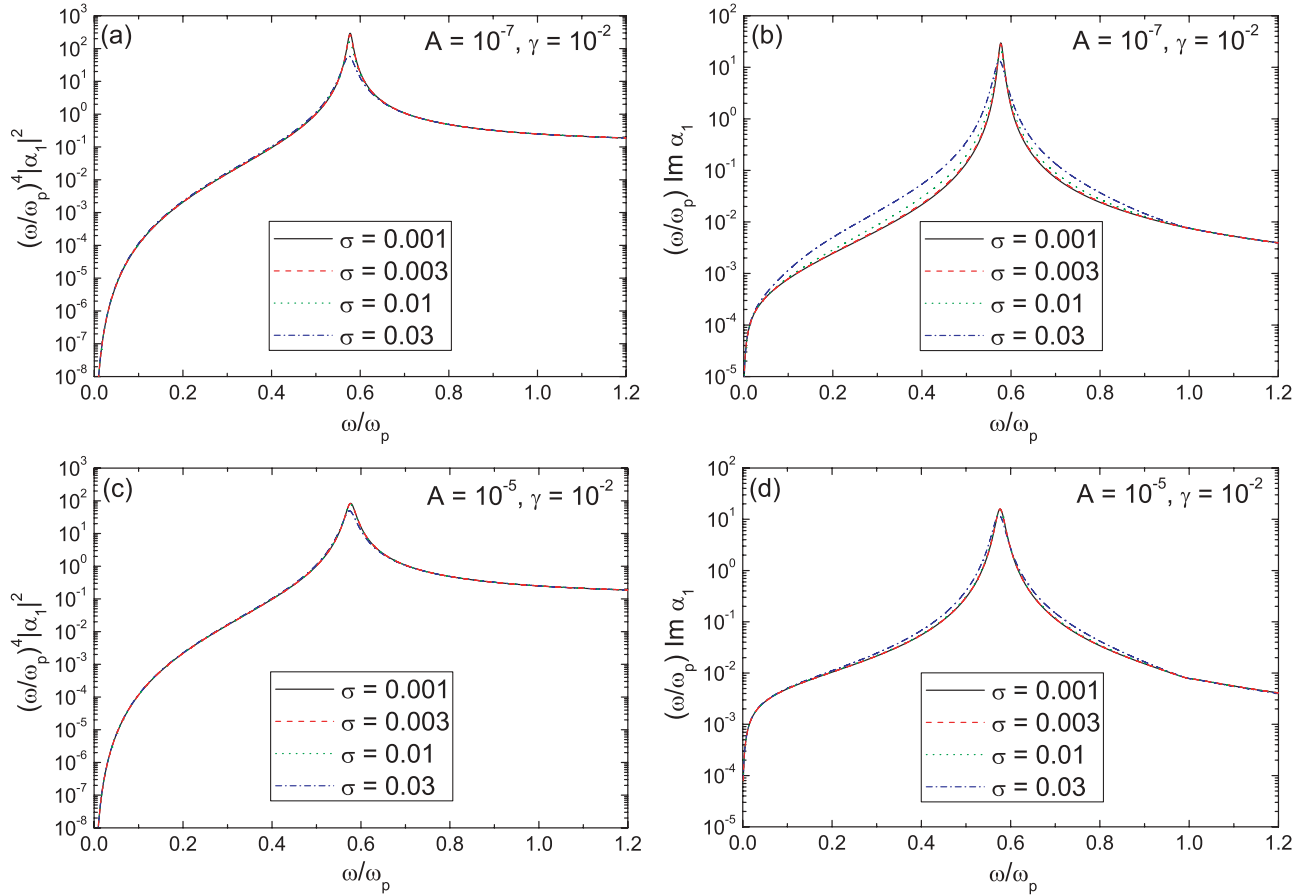
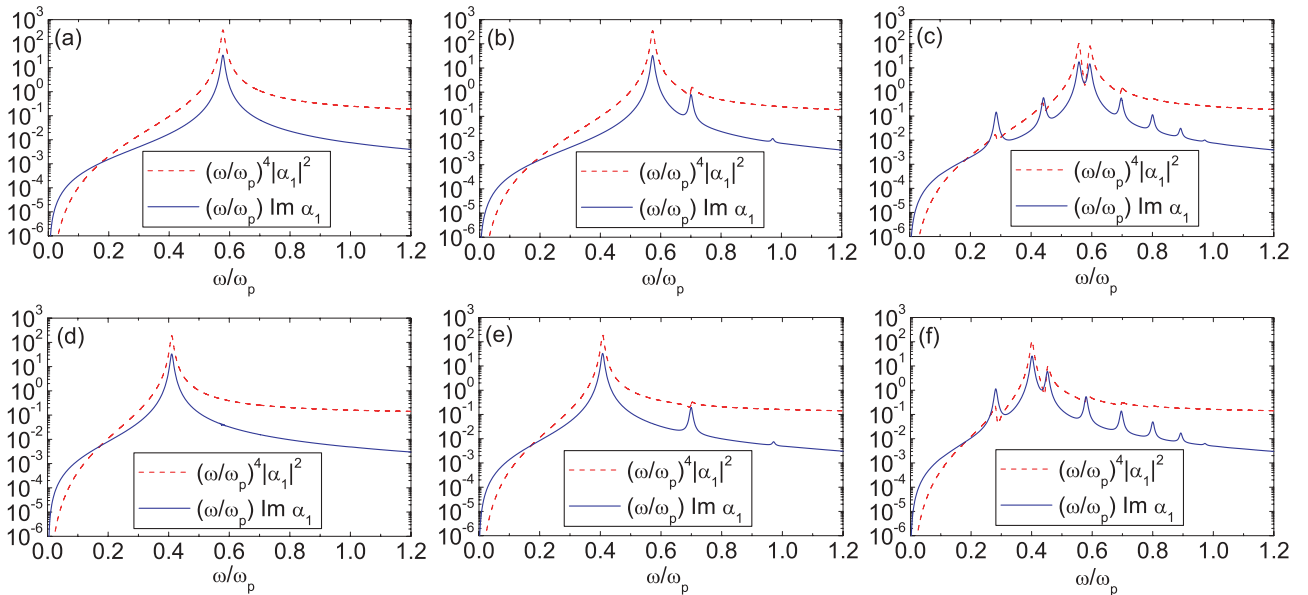

 FIG. 8. (Color online) The same as Fig. 7 but for $\gamma = 10^{-2}$.


FIG. 9. (Color online) The reduced cross sections of linear scattering and absorption, respectively, $\tilde{\omega}^4 |\alpha_1|^2$ and $\tilde{\omega} \text{Im} \alpha_1$, as a result of numerical solution of Eqs. (47) and (48) for cold neutral metal clusters without electron halo beyond the CCA ($A = 10^{-6}$) in vacuum [$\epsilon_1 = 1$, (a), (b), and (c)] and in a surrounding dielectric [$\epsilon_1 = 2$, (d), (e), and (f)], with $\gamma = 10^{-2}$ and for various cluster surface diffusenesses $\sigma/R = 0.003$ [(a) and (d)], $\sigma/R = 0.01$ [(b) and (e)], and $\sigma/R = 0.03$ [(c) and (f)]. For the ion density of the cluster surface region, the completely smooth profile $g_5(x)$ is used (see Fig. 1).

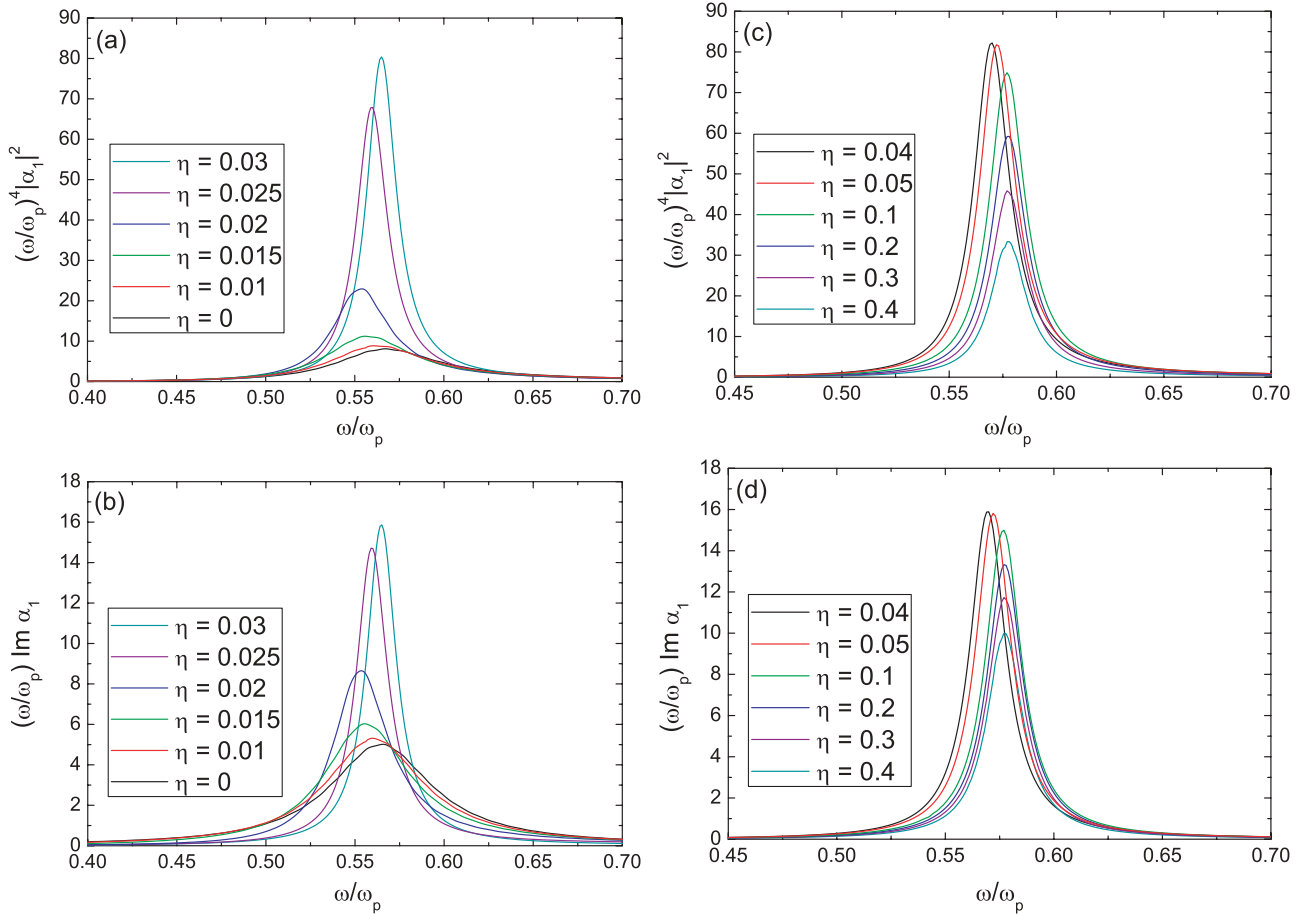


FIG. 10. (Color online) The reduced cross sections of linear scattering and absorption, respectively, $\tilde{\omega}^4 |\alpha_1|^2$ [(a) and (c)] and $\tilde{\omega} \text{Im} \alpha_1$ [(b) and (d)], as a result of the numerical solution of Eqs. (47) and (48) for a hot laser-heated/ionized cluster with an electron halo in vacuum ($\epsilon_1 = 1$) beyond the CCA ($A = 10^{-4}$) for $\sigma/R = 0.1$ and with $\gamma = 0.02$, and for various outer ionization degrees η . In (a) and (b), the six curves with increasing maxima correspond to the following increasing values of η : 0, 0.01, 0.015, 0.02, 0.025, 0.03, while in (c) and (d) the six curves with decreasing maxima correspond to the following increasing values of η : 0.04, 0.05, 0.1, 0.2, 0.3, 0.4. For the ion density of the cluster surface region, the completely smooth profile $g_5(x)$ is used (see Fig. 1). Increasing values of eta are bottom to top [(a) and (b)] and top to bottom [(c) and (d)].

In Figs. 7(a), 8(a), 7(b), and 8(b), the cluster parameter has the value $A = 10^{-7}$, while in Figs. 7(c), 8(c), 7(d), and 8(d) it is $A = 10^{-5}$. As was the case for $A = 0$ in the similar Fig. 3, in Figs. 7 and 8 the absorption as well as the scattering cross section reveal resonance behavior with a maximum at $\tilde{\omega} \approx 0.577$ for sufficiently small values of the relative cluster-surface thickness $\sigma/R \lesssim 0.001$, in precise agreement with the classical Mie-resonance frequency $\omega_M^{(cl)} = \omega_p/\sqrt{3}$ in vacuum. With σ/R increasing up to 0.03, a tiny red shift of the resonance frequency is observed. Also, with increasing σ/R , some broadening of the resonance curve takes place both for absorption and for scattering. For absorption, the cross section exhibits a significant increase on either side of the Mie-resonance frequency, restricted, however, to frequencies below the bulk plasma resonance frequency at $\tilde{\omega} = 1$. The physical reason for this enhancement is the same as explained above for the CCA. It is important to note that the magnitudes of both the scattering and the absorption cross sections for $A = 10^{-7}$ in Figs. 7 and 8 are only very slightly below those for $A = 0$ in Fig. 3. In contrast, with A increasing to 10^{-5} , these cross sections [Figs. 7(c), 8(c), 7(d), and 8(d)] are significantly

reduced by approximately one order of magnitude. It means that an increase of the parameter A , that is a decrease of the cluster radius, results in additional broadening of the resonance curves (in addition to already mentioned broadening due to increasing σ/R), both for the scattering and the absorption. The corresponding contribution to the resonance width is inversely proportional to the cluster radius. Moreover, due to this broadening at $A = 10^{-5}$ the effect of increasing σ/R is much less important. In conventional units, the width due to increasing A is proportional to $\omega_p \sqrt{A} = \omega_p l_Q/R \sim v_F/R$. This width is closely related to the one that appears in the kinetic approach as a consequence of the Landau damping mechanism in finite systems. In our approach it reveals itself already in the hydrodynamic approximation.

Figure 9 displays results obtained for a neutral cold metal cluster embedded into a surrounding dielectric beyond the CCA (for $A = 10^{-6}$), and for $\gamma = 10^{-2}$. For the calculations we set $\rho_{lim} = 1 + \sigma/(2R)$ in order to exclude the electron halo. Figures 9(a), 9(b), and 9(c) show the results for $\epsilon_1 = 1$ for comparison both with the previous results with the electron halo in vacuum and with the results for the surrounding

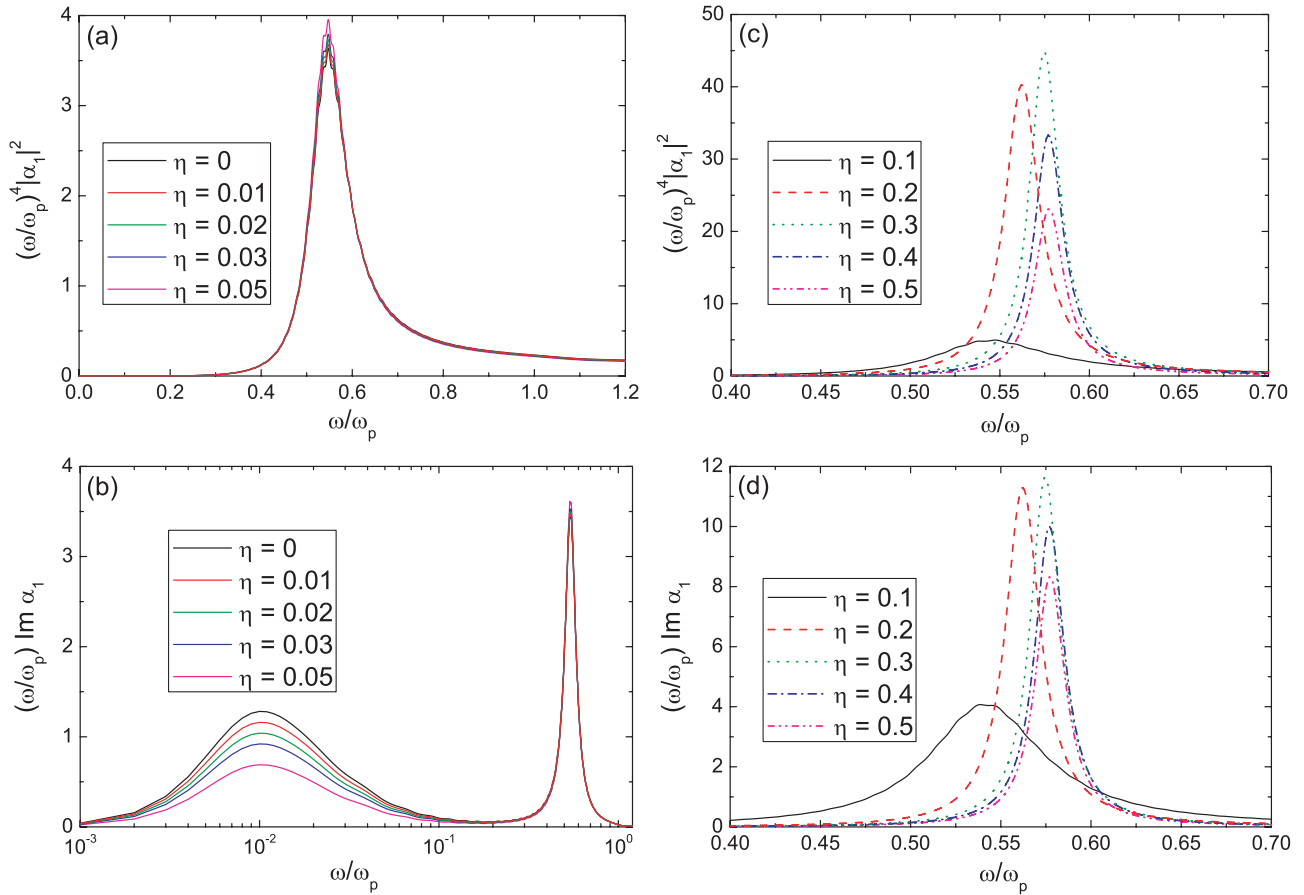


FIG. 11. (Color online) The reduced cross sections of linear scattering and absorption, respectively, $\tilde{\omega}^4 |\alpha_1|^2$ [(a) and (c)] and $\tilde{\omega} \text{Im} \alpha_1$ [(b) and (d)], as a result of the numerical solution of Eqs. (47) and (48) for a hot laser-heated/ionized cluster with an electron halo in vacuum ($\epsilon_1 = 1$) beyond the CCA ($A = 3 \times 10^{-3}$) for $\sigma/R = 0.03$ and with $\gamma = 0.02$ and for various outer ionization degrees η . In (a) and (b), the five curves with decreasing low-frequency maxima in absorption [(b)] correspond, respectively, to the following increasing values of η : 0, 0.01, 0.02, 0.03, 0.05, while in (c) and (d) the five curves correspond to the following values of η : 0.1 (solid curves), 0.2 (dashed curves), 0.3 (dotted curves), 0.4 (dashed-dotted curves), and 0.5 (dash-dot-dot curves). For the ion density of the cluster surface region, the completely smooth profile $g_5(x)$ is used (see Fig. 1). In (a) and (b), increasing values of eta are top to bottom.

permittivity $\epsilon_1 = 2$, which are exhibited in Figs. 9(d), 9(e), and 9(f). The main specific feature of these results both for $\epsilon_1 = 1$ (without the electron halo) and $\epsilon_1 = 2$ is the emergence of secondary resonances with increasing σ/R below the nominal plasma resonance frequency $\tilde{\omega} = 1$, especially in absorption, along with the basic Mie resonance, which remains present both in scattering and in absorption. These secondary resonances are absent for low $\sigma/R \lesssim 0.003$. They gradually appear in increasing numbers with increasing relative surface diffuseness. Figure 9 also shows that the basic Mie resonance shifts toward lower frequencies with increasing permittivity ϵ_1 of the surrounding dielectric, while the secondary resonance frequencies are less affected by increasing ϵ_1 . The position of the basic Mie resonance is in rather good qualitative agreement with the classical Mie-resonance frequency in a dielectric, $\omega_M^{(cl)} = \omega_p / \sqrt{1 + 2\epsilon_1}$ [10,67], which is obtained in the electrostatic approximation. Quantitatively, however, the basic Mie-resonance frequency obtained in our calculations at $\epsilon_1 = 2$ is in excellent quantitative agreement ($\tilde{\omega}_M \approx 0.41$) with the plasmon Mie-resonance frequency $\omega_M = \omega_p / \sqrt{3\epsilon_1}$ derived above on the basis of the CCA. The secondary resonances that appear with increasing surface diffuseness of

the cluster qualitatively can be interpreted as the well-known Tonks-Dattner resonances below the plasma frequency in a uniform bounded plasma, which are due to the nonuniformity of the edge [68,69].

Figure 10 exhibits the results obtained for a charged cluster in vacuum ($\epsilon_1 = 1$) beyond the CCA ($A = 10^{-4}$) with electron halo, for $\gamma = 0.02$ and $\sigma/R = 0.1$ and for different values of the outer-ionization degree η . In this case, in the CCA the critical value of the outer-ionization degree, which separates the ranges of low and high ionization degrees with respect to electron depletion of the diffuse cluster surface, is $\eta_c \approx 0.14$ [cf. Eq. (44)]. Beyond the CCA, the electron halo should play a significant role for low ionization degree as well as for a neutral cluster, while for high ionization degree the halo effect is depressed by the Coulomb trapping of the residual electrons inside the cluster. Figure 10 illustrates the behavior of the resonance curves for the current case beyond the CCA with an electron halo upon variation of η , for a cluster at low ionization degree $\eta \leq 0.03$ in Figs. 10(a) and 10(b) as compared with a charged cluster at high outer-ionization degree $\eta \geq 0.04$ in Figs. 10(c) and 10(d). Both for scattering [Fig. 10(a)] and for absorption [Fig. 10(b)], the resonance

curves narrow and the magnitude of the Mie resonance increases when η is increasing up to approximately 0.04. When η continues to increase up to 0.4 in Figs. 10(c) and 10(d), the magnitude of the resonance starts to decrease again. For charged clusters and nonzero η , the position of the Mie resonance is always red-shifted with respect to the classical Mie-resonance frequency in vacuum, $\tilde{\omega}_M^{(cl)} = 1/\sqrt{3}$. However, the magnitude of the shift depends nonmonotonically on η : with η increasing from zero, the shift first increases. It reaches a maximum at about $\eta = 0.02$ and thereafter decreases again, ultimately to reach the limit of the classical position for high ionization degrees.

Finally, Fig. 11 shows results obtained for several different values of the outer-ionization degree η for a charged cluster in vacuum ($\epsilon_1 = 1$) with an electron halo beyond the CCA at a higher value of the cluster parameter $A = 3 \times 10^{-3}$, for $\gamma = 0.02$ and $\sigma/R = 0.03$. Though at high ionization degrees [see Figs. 11(c) and 11(d)] the evolution of the Mie-resonance curves is qualitatively the same as in the previous case of Fig. 10, a new specific feature of this case is the appearance of a rather significant additional low-frequency maximum in the absorption [see Fig. 11(b)] at low ionization degrees, whose magnitude gradually disappears with increasing outer-ionization degree. For $\eta \geq 0.1$, this low-frequency maximum in the absorption is negligible, and it does not manifest itself at all in the scattering cross section. It was also present in the previous case of Fig. 10 with $A = 10^{-4}$ but only as a very small effect. Though apparently it is not a numerical artifact, the physical reason for the appearance of this low-frequency peak in the absorption is not completely clear. But very clearly its existence is tightly connected with the presence of an electron halo, whose role is also reduced with increasing outer-ionization degree.

V. CONCLUSIONS

In this article, the collisionless hydrodynamic model for both the linear and the nonlinear electron response of a small free-electron nanocluster with diffuse boundary to the action of linearly polarized laser light has been developed. The nonlinearity is introduced through the basic nonlinearity of the charge-field interaction and through the convective derivative in the equation of motion. Corresponding nonlinearities naturally exist in the hydrodynamic equations. The effect of the nonlinearities is especially pronounced in the cluster boundaries owing to the corresponding short-scale variation in the electron density, the electric field, and the electron velocity. Both cold metal nanoclusters and hot laser-heated and/or ionized nanoclusters can be analyzed in detail in the framework of the same approach. In order to use analytical methods as far as possible in this from the numerical point of view very stiff problem, the stationary approximation as well as perturbation theory are used. In addition, the ions are considered frozen. This gives the possibility to restrict the study to the response of the electron subsystem of the nanocluster and to investigate the laser-frequency dependence of scattering and absorption. Two different perturbation expansions were distinguished in this context. One of them corresponds to sufficiently high laser fields, when the amplitude of the forced electron oscillations inside the cluster is smaller

than the thickness of the diffuse boundary but still larger than the electric charge separation. The other is applicable for lower laser fields, when the amplitude of the forced electron oscillations inside the cluster is even smaller than the electric charge separation. This cluster model is developed on the basis of the similar one-dimensional collisionless hydrodynamic model that was presented in Ref. [60] and applied to thin nanofilms interacting with p -polarized laser light.

The main interest of the ongoing study will be concerned with nonlinear effects and, in particular, a detailed study of third-harmonic generation by a free-electron nanocluster with diffuse boundary. However, the linear cluster response is at the base of the consideration of the nonlinear problems, and in itself already constitutes a formidable problem. Therefore, in this first article, having developed the complete nonlinear model, we have restricted ourselves to the linear electromagnetic nanocluster response, when it came to the presentation of detailed results. We have considered both scattering and absorption of the incident laser light, for different scenarios of the irradiated cluster, such as cold clusters, hot clusters, neutral or charged clusters, clusters in the presence of a dielectric environment or in vacuum, with or without an electron halo surrounding the cluster, and so on. In particular, we have shown that for frequencies below the nominal plasma frequency, linear absorption in a small nanocluster with diffuse surface can be much higher than for a similar cluster with a sharp steplike boundary. For a cold cluster in a dielectric environment, a small but noticeable red shift of the Mie-resonance frequency with respect to its classical value $\tilde{\omega}_M^{(cl)} = \sqrt{1 + 2\epsilon_1}$ was obtained, and this shift depends on the dielectric permittivity of the environment. It was shown analytically that the correct value of the Mie-resonance frequency of the cluster in the dielectric environment with permittivity ϵ_1 corresponds to the expression $\sqrt{3\epsilon_1}$ rather than to $\sqrt{1 + 2\epsilon_1}$, which follows from the electrostatic approximation. It was shown that in our hydrodynamic model the width of the Mie resonance depends both on the thickness of the diffuse boundary as well as on the cluster radius (this occurred through the presence of the cluster parameter A , provided we did not invoke the CCA). For cold neutral metal nanoclusters and moderate laser fields, we also found that the frequency dependence of the linear absorption exhibits secondary resonances along with the main Mie-resonance peak. In our model, the number of such secondary absorption peaks increases with increasing cluster boundary thickness. In contrast, for hot laser-heated clusters in vacuum the extra resonances in the linear absorption do not appear, except for the additional low-frequency maximum at a high value of A . On the other hand, the outer-ionization degree significantly affects the resonance profile of both linear absorption and linear scattering for hot charged clusters in vacuum. This is also tightly connected both with the cluster boundary effect and with the electron halo due to the strong dependence of the nonuniform electron density in the near-surface range on the outer-ionization degree.

For the nonlinear effects, the corresponding equations and calculations are much more cumbersome than in the linear case. High-order harmonic generation by the cluster can hardly be considered in this context on the

basis of perturbation theory, but for third-harmonic generation it is still feasible. The detailed numerical study of third-harmonic generation and the first nonlinear correction to laser absorption by free-electron nanoclusters with diffuse surface will be the subject of a following separate article.

ACKNOWLEDGMENTS

This work was supported by the Deutsche Forschungsgemeinschaft [Project No. 436 RUS 113/852/0-1(R)] and by the Russian Foundation for Basic Research (Grant No. 09-02-00773-a).

-
- [1] J. W. Strutt, *Phil. Mag. Ser. 4* **41**, 447 (1871).
- [2] G. Mie, *Ann. Phys. (Leipzig)* **25**, 377 (1908).
- [3] Ph. J. Wyatt, *Phys. Rev.* **127**, 1837 (1962).
- [4] R. Ruppin, *Phys. Rev. Lett.* **31**, 1434 (1973).
- [5] R. Ruppin, *Phys. Rev. B* **11**, 2871 (1975).
- [6] R. Ruppin, *J. Opt. Soc. Am.* **66**, 449 (1976).
- [7] R. Ruppin, *J. Phys. Chem. Solids* **39**, 233 (1978).
- [8] A. G. Lesskis, V. E. Pasternak, and A. A. Yushkanov, *Sov. Phys. JETP* **56**, 170 (1982) [*Zh. Eksp. Teor. Fiz.* **83**, 310 (1982)].
- [9] H. C. van de Hulst, *Light Scattering by Small Particles* (Dover, New York, 1981).
- [10] C. F. Bohren and D. R. Huffman, *Absorption and Scattering of Light by Small Particles* (Wiley, New York, 1983).
- [11] W. Ekardt, *Phys. Rev. B* **31**, 6360 (1985).
- [12] V. Kresin, *Phys. Lett. A* **133**, 89 (1988).
- [13] V. Kresin, *Phys. Rev. B* **39**, 3042 (1989).
- [14] V. Kresin, *Phys. Rev. B* **42**, 3247 (1990).
- [15] V. Kresin, *Z. Phys. D* **19**, 105 (1991).
- [16] V. V. Kresin, *Phys. Rep.* **220**, 1 (1992).
- [17] A. Rubio, L. C. Balbás, and J. A. Alonso, *Z. Phys. D* **19**, 93 (1991).
- [18] J. Kupersztych and M. Raynaud, *J. Phys. Condens. Matter* **6**, 10669 (1994).
- [19] U. Kreibig and M. Vollmer, *Optical Properties of Metal Clusters* (Springer, Berlin, 1995).
- [20] F. Calvayrac, P.-G. Reinhard, and E. Suraud, *J. Phys. B: At. Mol. Opt. Phys.* **31**, 1367 (1998).
- [21] S. V. Fomichev and D. F. Zaretsky, *J. Phys. B: At. Mol. Opt. Phys.* **32**, 5083 (1999).
- [22] P.-G. Reinhard and E. Suraud, *Introduction to Cluster Dynamics* (Wiley, Berlin, 2003).
- [23] A. M. Bystrov and V. B. Gildenburg, *JETP* **100**, 428 (2005) [*Zh. Eks. Teor. Fiz.* **127**, 478 (2005)].
- [24] D. Débarre, N. Olivier, and E. Beaurepaire, *Opt. Express* **15**, 8913 (2007).
- [25] C.-F. Chang, C.-Y. Chen, F.-H. Chang, S.-P. Tai, C.-Y. Chen, C.-H. Yu, Y.-B. Tseng, T.-H. Tsai, I.-S. Liu, W.-F. Su, and C.-K. Sun, *Opt. Express* **16**, 9534 (2008).
- [26] K. E. Sheetz and J. Squier, *J. Appl. Phys.* **105**, 051101 (2009).
- [27] F. Hache, D. Ricard, and C. Flytzanis, *J. Opt. Soc. Am. B* **3**, 1647 (1986).
- [28] X. M. Hua and J. I. Gersten, *Phys. Rev. B* **33**, 3756 (1986).
- [29] K. Hayata and M. Koshihara, *Phys. Rev. A* **46**, 6104 (1992).
- [30] D. Östling, P. Stampfli, and K. H. Bennemann, *Z. Phys. D* **28**, 169 (1993).
- [31] J. P. Dewitz, W. Hübner, and K. H. Bennemann, *Z. Phys. D* **37**, 75 (1996).
- [32] K. Hagino, *Phys. Rev. B* **60**, R2197 (1999).
- [33] L. G. Gerchikov, C. Guet, and A. N. Ipatov, *Phys. Rev. A* **66**, 053202 (2002).
- [34] J.-P. Connerade and A. V. Solovyov, *Phys. Rev. A* **66**, 013207 (2002).
- [35] S. V. Fomichev, S. V. Popruzhenko, and D. F. Zaretsky, *Laser Physics* **13**, 1188 (2003).
- [36] S. V. Fomichev, S. V. Popruzhenko, D. F. Zaretsky, and W. Becker, *J. Phys. B: At. Mol. Opt. Phys.* **36**, 3817 (2003).
- [37] S. V. Fomichev, S. V. Popruzhenko, D. F. Zaretsky, and W. Becker, *Opt. Express* **11**, 2433 (2003).
- [38] S. V. Fomichev, D. F. Zaretsky, and W. Becker, *J. Phys. B: At. Mol. Opt. Phys.* **37**, L175 (2004).
- [39] S. V. Fomichev, D. F. Zaretsky, D. Bauer, and W. Becker, *Phys. Rev. A* **71**, 013201 (2005).
- [40] B. N. Breizman and A. V. Arefiev, *Plasma Phys. Rep.* **29**, 593 (2003) [*Fiz. Plazmy* **29**, 642 (2003)].
- [41] M. V. Fomytskyi, B. N. Breizman, A. V. Arefiev, and Ch. Chiu, *Phys. Plasmas* **11**, 3349 (2004).
- [42] B. N. Breizman, A. V. Arefiev, and M. V. Fomytskyi, *Phys. Plasmas* **12**, 056706 (2005).
- [43] V. I. Shcheslavskiy, S. M. Saltiel, A. Faustov, G. I. Petrov, and V. V. Yakovlev, *J. Opt. Soc. Am. B* **22**, 2402 (2005).
- [44] S. V. Popruzhenko, D. F. Zaretsky, and W. Becker, *J. Phys. B: At. Mol. Opt. Phys.* **39**, 4933 (2006).
- [45] P. K. Tiwari and V. K. Tripathi, *Phys. Scr.* **74**, 682 (2006).
- [46] M. Kundu, S. V. Popruzhenko, and D. Bauer, *Phys. Rev. A* **76**, 033201 (2007).
- [47] S. V. Popruzhenko, M. Kundu, D. F. Zaretsky, and D. Bauer, *Phys. Rev. A* **77**, 063201 (2008).
- [48] S. V. Popruzhenko, D. F. Zaretsky, and D. Bauer, *Laser Phys. Lett.* **5**, 631 (2008).
- [49] Ph. A. Korneev, S. V. Popruzhenko, D. F. Zaretsky, and W. Becker, *Laser Phys. Lett.* **2**, 452 (2005).
- [50] P. Mulser, M. Kanopathipillai, and D. H. H. Hoffmann, *Phys. Rev. Lett.* **95**, 103401 (2005).
- [51] P. Mulser and M. Kanopathipillai, *Phys. Rev. A* **71**, 063201 (2005).
- [52] M. Kundu and D. Bauer, *Phys. Rev. Lett.* **96**, 123401 (2006).
- [53] M. Kundu and D. Bauer, *Phys. Rev. A* **74**, 063202 (2006).
- [54] A. R. Holkundkar and N. K. Gupta, *Phys. Plasmas* **15**, 013105 (2008).
- [55] A. R. Holkundkar and N. K. Gupta, *Contrib. Plasma Phys.* **49**, 403 (2009).
- [56] M. Lippitz, M. A. van Dijk, and M. Orrit, *Nano Lett.* **5**, 799 (2005).
- [57] M. A. van Dijk, M. Lippitz, and M. Orrit, *Acc. Chem. Res.* **38**, 594 (2005).
- [58] T.-M. Liu, S.-P. Tai, C.-H. Yu, Y.-C. Wen, S.-W. Chu, L.-J. Chen, M. R. Prasad, K.-J. Lin, and C.-K. Sun, *Appl. Phys. Lett.* **89**, 043122 (2006).
- [59] B. Shim, G. Hays, R. Zgadzaj, T. Ditmire, and M. C. Downer, *Phys. Rev. Lett.* **98**, 123902 (2007).

- [60] S. V. Fomichev, D. F. Zaretsky, and W. Becker, *Phys. Rev. B* **79**, 085431 (2009).
- [61] S. I. Braginskii, in *Reviews of Plasma Physics*, edited by M. A. Leontovich (Consultants Bureau, New York, 1965), Vol. I, p. 205.
- [62] V. P. Silin, *Vvedenie v Kineticheskuyu Teoriyu Gazov* (Introduction to the Kinetic Theory of Gases) (Nauka, Moscow, 1971) [in Russian].
- [63] E. M. Lifshitz and L. P. Pitaevsky, *Course of Theoretical Physics, Vol. X, Physical Kinetics* (Pergamon, Oxford, 1981).
- [64] M. Kanopathipillai, P. Mulser, D. H. H. Hoffmann, T. Schlegel, Y. Maron, and R. Sauerbrey, *Phys. Plasmas* **11**, 3911 (2004).
- [65] J. D. Jackson, *Classical Electrodynamics*, 3rd ed. (Wiley, New York, 1999).
- [66] P. Gibbon, *Short Pulse Laser Interactions with Matter* (Imperial College Press, London, 2005).
- [67] L. D. Landau, E. M. Lifshitz, and L. P. Pitaevskii, *Course of Theoretical Physics, Vol. VIII, Electrodynamics of Continuous Media*, 2nd ed. (Butterworth-Heinemann, Oxford, 1984).
- [68] L. Tonks, *Phys. Rev.* **37**, 1458 (1931).
- [69] A. Dattner, *Ericsson Technics* **2**, 309 (1957); **8**, 1 (1963).